



## A Flow-Driven Cavity as an Air Cycling Model for Window Flow

Justin Campbell

Amanda Hiett

Akhil Sadam

---

### Abstract

A lid-driven cavity is flow-driven to describe stress on and circulation inside buildings and small insect-to-UAV-size aircraft due to open windows or sidewall punctures. The transition between steady & unsteady flow is also roughly bounded, by investigating the Reynolds number at 4 values between 10 to  $10^4$ . A sparse simulation of low-speed and much higher-speed incompressible flows is undertaken, estimating feature shapes at the minimum computational cost.

*Keywords:* computational fluid dynamics, CFD, incompressible, Paraview, R, Python, coe347, spring 2022, window, building, tornado, high, reynolds, unsteady, steady, stress, strain, rate, mixing, volumetric, flow.

---

### 1. Motivation

For severe storms, it is widely known that puncture damage is the primary cause of failure for most buildings and aircraft. Once a puncture has been created, the resultant pressure differential can cause fast inflow and damage to the interior. We seek to study this inflow, and stresses near the opening walls, which can cause structural issues leading to collapse of one or more walls.

Most relevant studies use incredibly large amounts of computational power, due to the large scale of the problem (Reynolds numbers for tornadoes and hurricanes can easily start in the millions). We seek to show the applicability of lower Reynolds simulations to higher Reynolds situations, since the general large-scale flow structure remains the same.

### 2. Implementation

We implement all simulation with OpenFoam, analysis with Paraview and Python3, and documentation code in R [Xie, Dervieux, and Riederer \(2020\)](#).

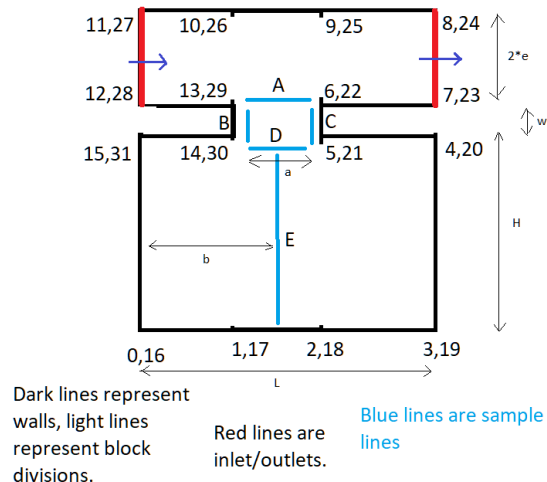
### **3. Mesh Assembly**

We assembled a 2D mesh template as below, with the following parameters, all lengths nondimensionalized in terms of dimension  $L$ :

mutable: wall thickness  $w$ , window width  $a$ ,

immutable: window location  $b = 0.5$ , cavity height  $H = 1$ , cavity width  $L = 1$ , and free-stream width  $2e = 0.1$ .

## BlockMesh Diagram



Two sets of simulations are performed, one for the low Reynolds ( $Re$ ) numbers of 10 and 200, which will be shown to be steady, and another for  $Re = 1000, 10000$ .

Each mesh also has a corresponding refinement, which is described by the *meshFactor* parameter, representing the refinement in each dimension.

Full lists are available below.

### 3.1. Meshes for the Low Reynolds simulations

<b>meshfactor</b>	<b>Reynolds</b>	<b>a</b>	<b>w</b>
5	10	0.05	0.05
5	10	0.05	0.10
5	10	0.50	0.05
5	10	0.50	0.10
10	10	0.05	0.05
10	10	0.05	0.10
10	10	0.50	0.05
10	10	0.50	0.10
5	200	0.05	0.05
5	200	0.05	0.10
5	200	0.50	0.05
5	200	0.50	0.10
10	200	0.05	0.05
10	200	0.05	0.10
10	200	0.50	0.05
10	200	0.50	0.10

Table 1:

**3.2. Meshes for the High Reynolds simulations**

<b>meshfactor</b>	<b>Reynolds</b>	<b>a</b>	<b>w</b>
3	1000	0.5	0.1
5	1000	0.5	0.1
3	10000	0.5	0.1
5	10000	0.5	0.1

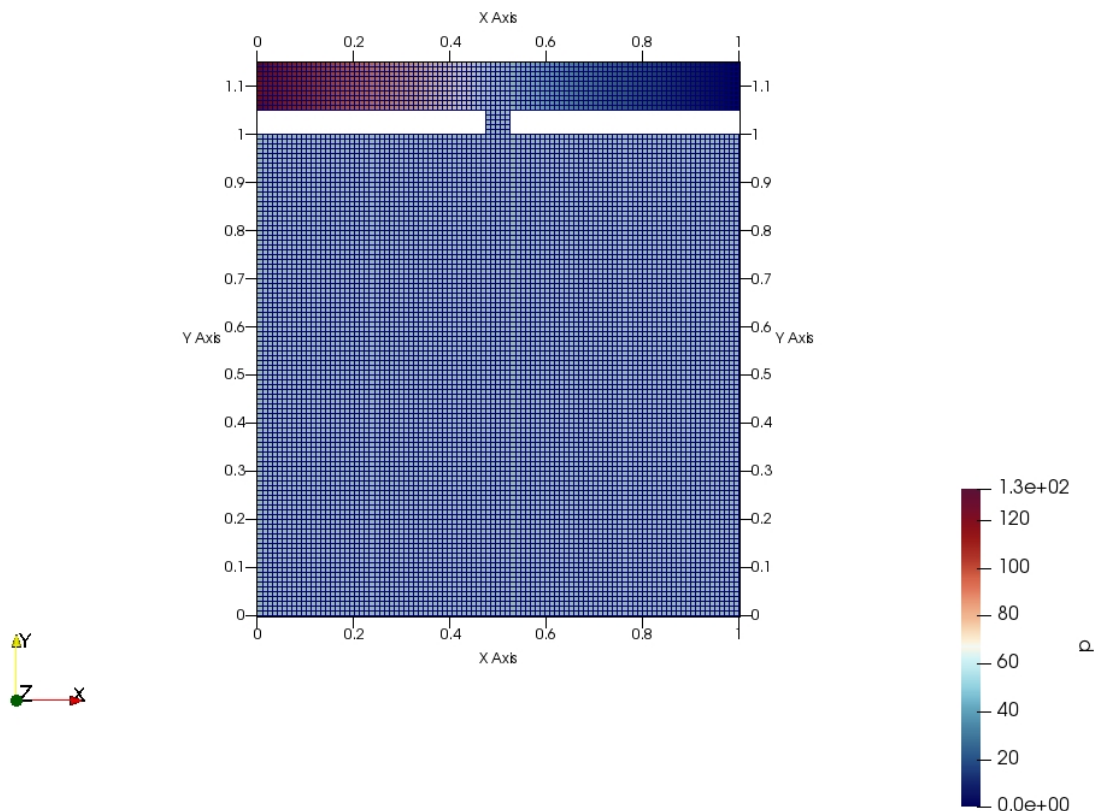
Table 2:

BlockMeshDict and similar files are available at [the repository](#).

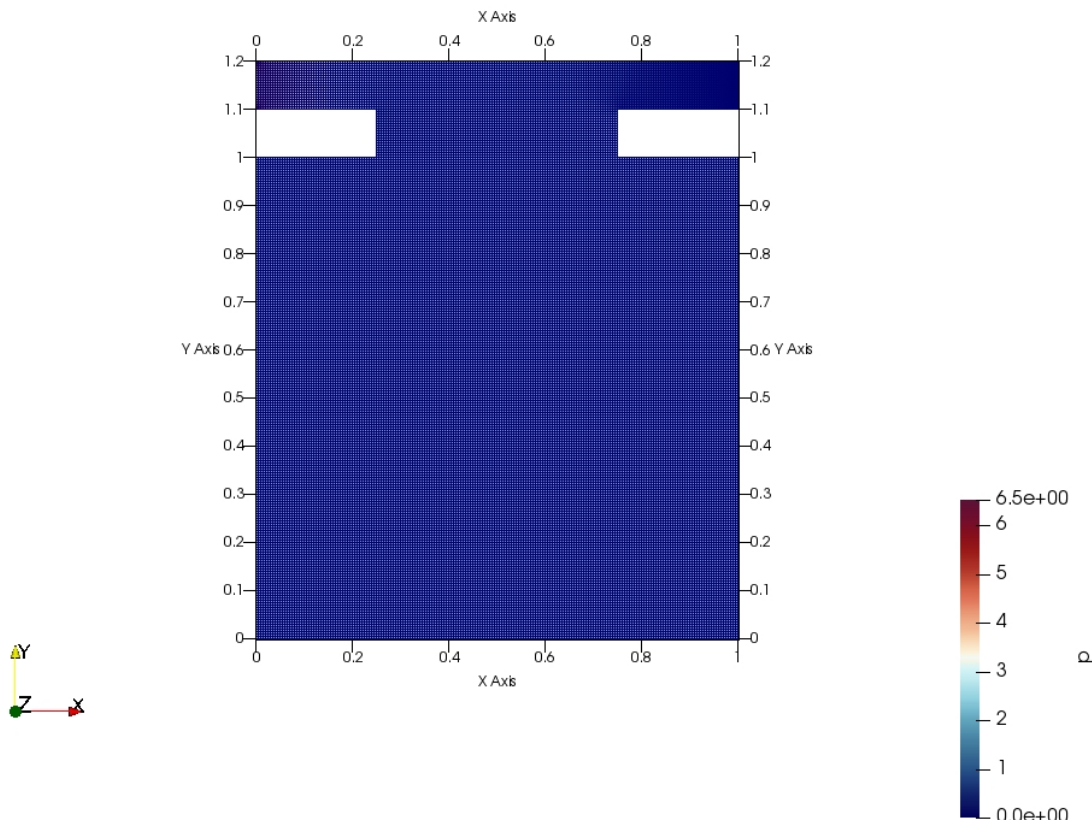
**3.3. Mesh Images**

A couple mesh samples are shown here; see the appendix for all images.

meshFactor, Re, windowWidth, wallThickness=5, 10, 0.05, 0.05:



meshFactor, Re, windowWidth, wallThickness=10, 200, 0.5, 0.1:



Now that the mesh resolutions can be seen as adequate, we will move to results.

#### 4. Literature Review

Wind speeds may be categorized as dangerous once reaching the threshold of 50mph. Winds of this caliber may occur during storms and tornados, and can be catastrophic to infrastructure.(2019; Hadhazy 2011; Tessner 2021)

Structurally, windows are weak in comparison to the surrounding structure and therefore are generally the first to break when confronted with strong winds. The missing window then creates a cavity with a pressure differential to the outside wind that may encourage further destruction. The fragility of windows is why many coastal buildings near hurricane hotspots have shutters, and in the event of a storm, those without shutters often cover their windows with materials such as plywood to protect against the oncoming winds.(2019; Hadhazy 2011; Tessner 2021)

The average home is designed to withstand winds of 90mph for around 3 seconds, which is far from sufficient to withstand even a moderate class of tornado. Especially when including forces working in tandem generating lift on top of normal stressors. As roof connections rely primarily on gravity to ensure stability, any opposing force to gravity need only overcome the weight force of the roof to remove it from the structure entirely.(2019; Hadhazy 2011; Tessner 2021)

Due to the propensity of air to create vortices when exposed to nonzero velocity and pressure differential, the way air may travel through the structure could pose an additional destructor on top of the exterior conditions. It has been proven advantageous for homes in storm-prone areas to install shutters, so prevention of inducing cavity-like flow on a structure is of import.(2019; Hadhazy 2011; Tessner 2021)

## 5. Low Reynolds Number

Low Reynolds numbers are generally indicative of laminar airflow and low airspeeds. Although storm winds do not fall into this category, it is useful to examine the behavior of the airflow at low speeds to gauge the general effects of altering physical parameters such as wall thickness and window width. Windows come in a variety of sizes, as do wall thicknesses - so it is important to understand the effects of altering the aforementioned geometries on the airflow.

Note all values are nondimensionalized - all lengths are in terms of  $L$ , the cavity length, all speeds in terms of  $U$ , the initial flow speed, and all times in terms of  $\frac{L}{U}$ .

The pressure is in terms of  $\frac{p}{\rho U^2}$ . All low-Reynolds simulations were run till T=6.

### 5.4. General Solution Form

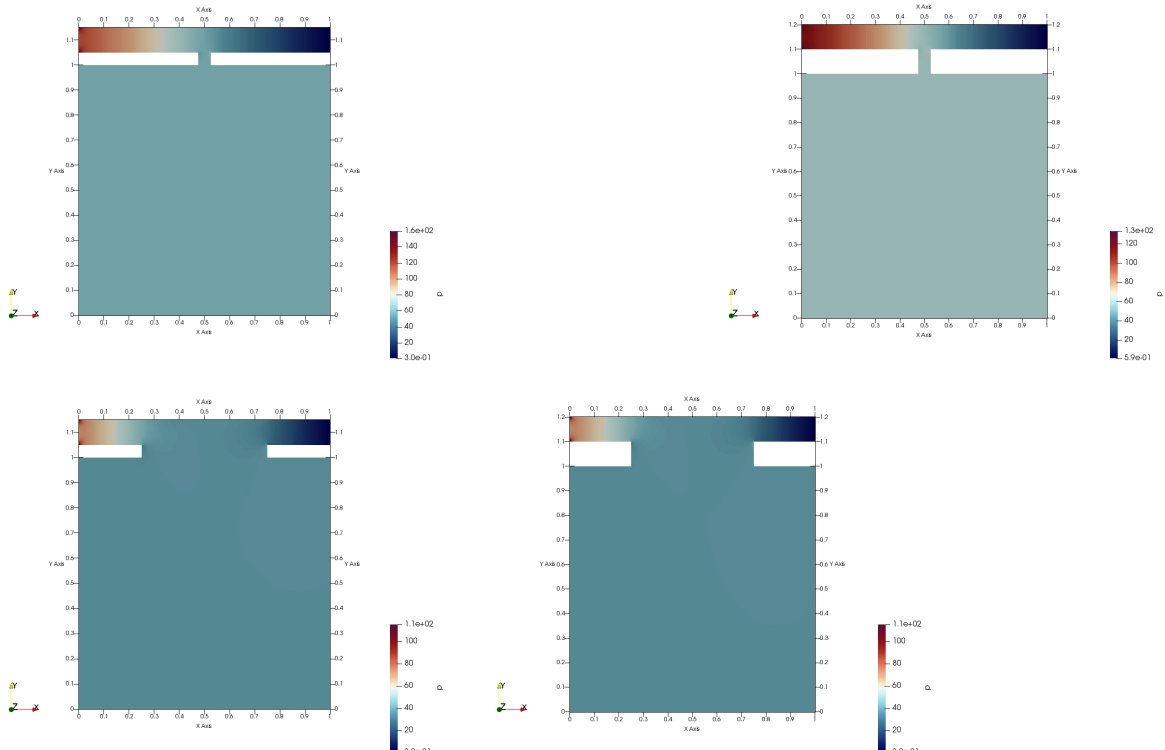
We will now show the pressure, X-velocity, Y-velocity, and streamlines in sets of 4 by varying geometry along the following pattern. Contours are not shown due to their bias toward out-of-cavity portions and the coarse mesh will be omitted for brevity. Convergence studies will be done numerically afterward.

Pattern:

window.size.a wall.thickness.w	
0.05	0.05
0.05	0.10
0.50	0.05
0.50	0.10

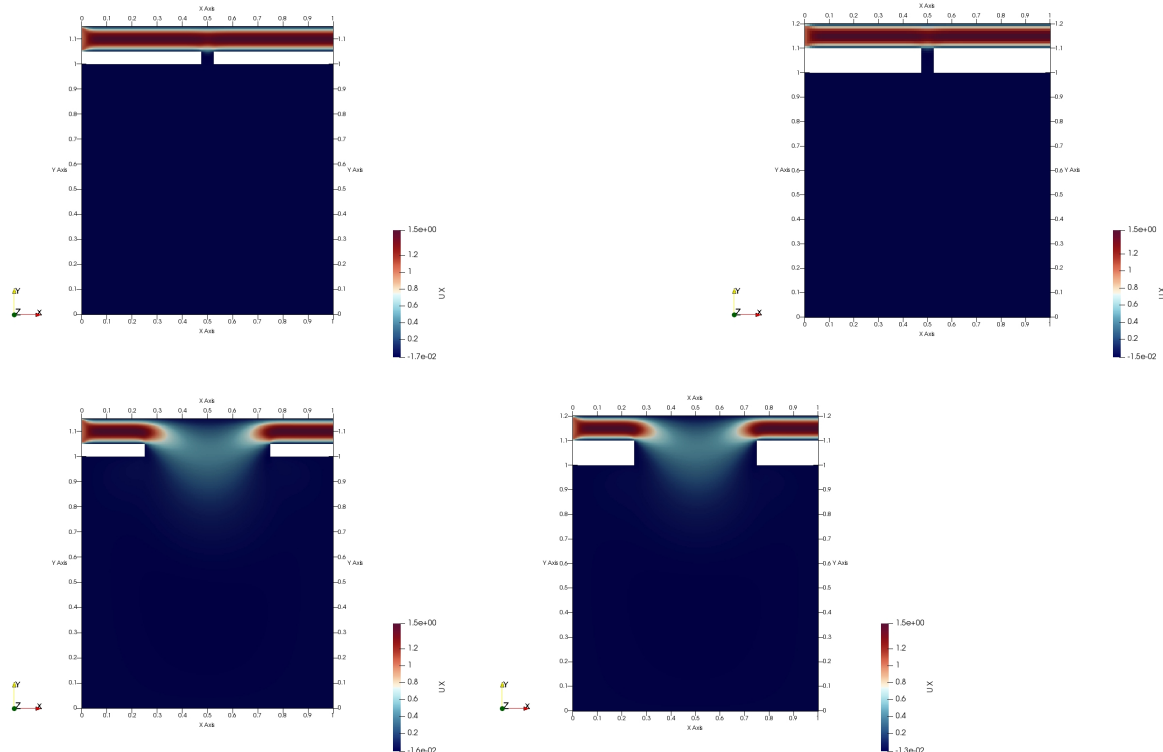
Table 3:

### Re=10, Pressure



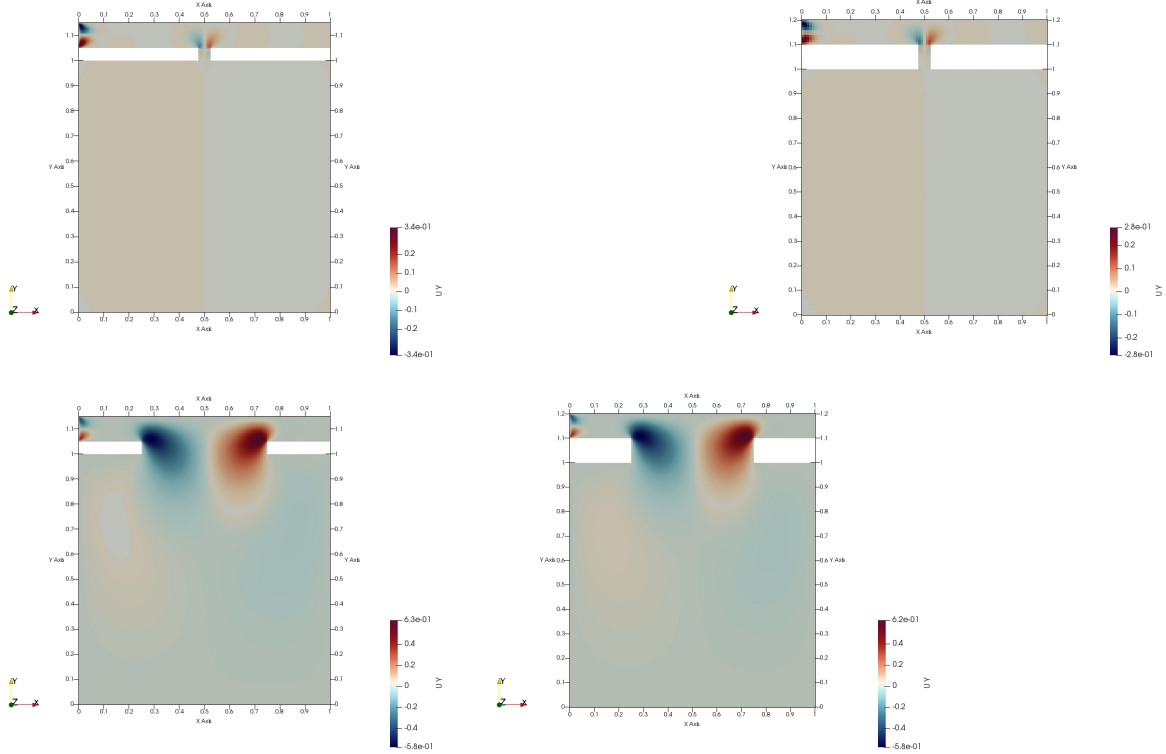
Note that all meshes have relatively even internal pressure, suggesting internal flow speeds are minuscule. Also, the more contact the cavity has with the crossflow, the lower the internal cavity pressure. This pressure differential works in attempt to equalize flow conditions, but due to the gradient induced by unequal flows, the interior pressure drops. Finally, consider the inlet. Note that the higher-pressure regions localize at the corners with larger windows, implying that the cavity acts as a sort of pressure sink.

### Re=10, X-velocity



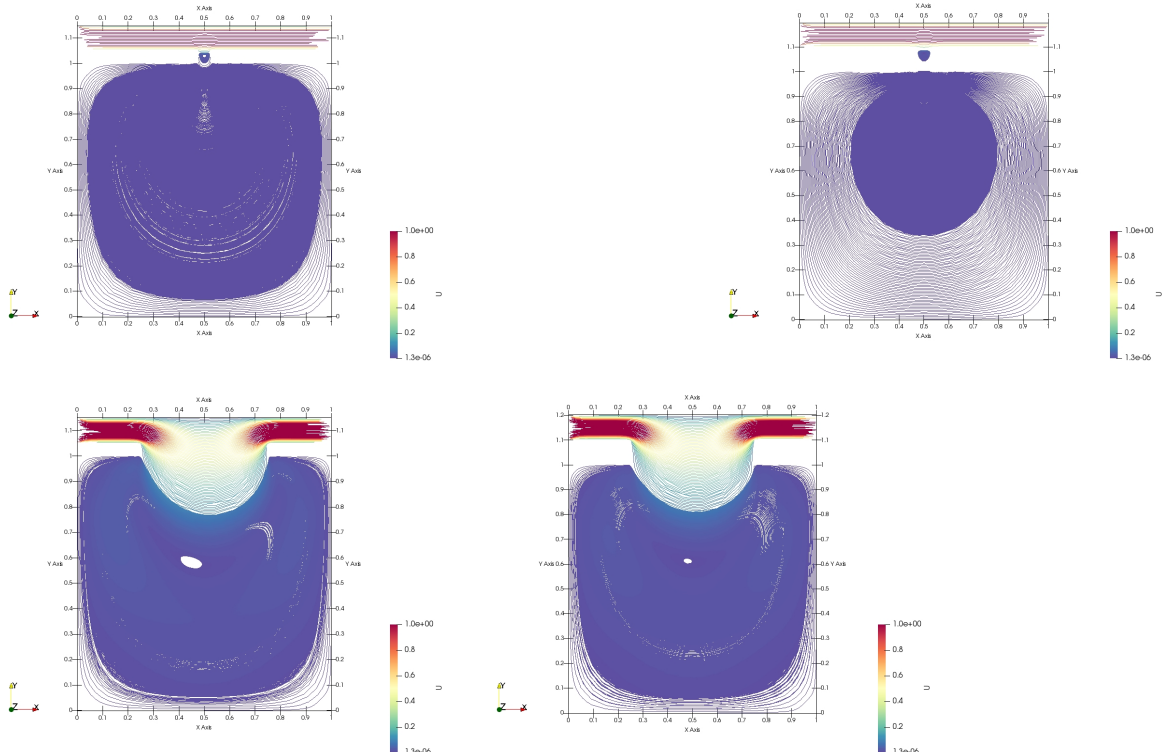
Similarly, the flow x-velocity dissipates across the window in amounts positively correlated with larger and thinner windows. This is due to the reduced physical impedance of an impermeable zero-flow velocity structure that is the wall. No discernible cavity flow can be seen yet.

### Re=10, Y-velocity



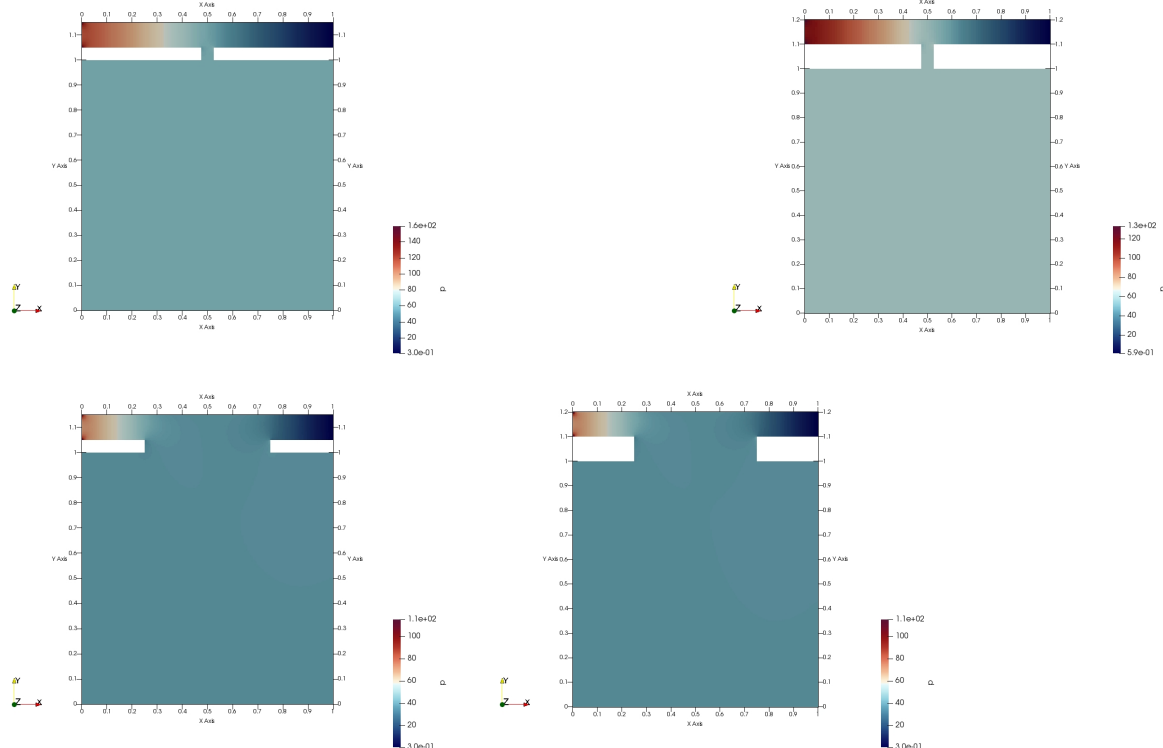
The same story can be seen in the  $y$ -velocities, but now there can be seen a cavity circulation (by the mild color differences inside the cavity). Note that the windows of 0.05 width produce really mild, near-complete cavity circulation, while the larger windows of 0.5 width produce much stronger but incomplete circulation (the corners are relatively unaffected).

## Re=10, Streamlines



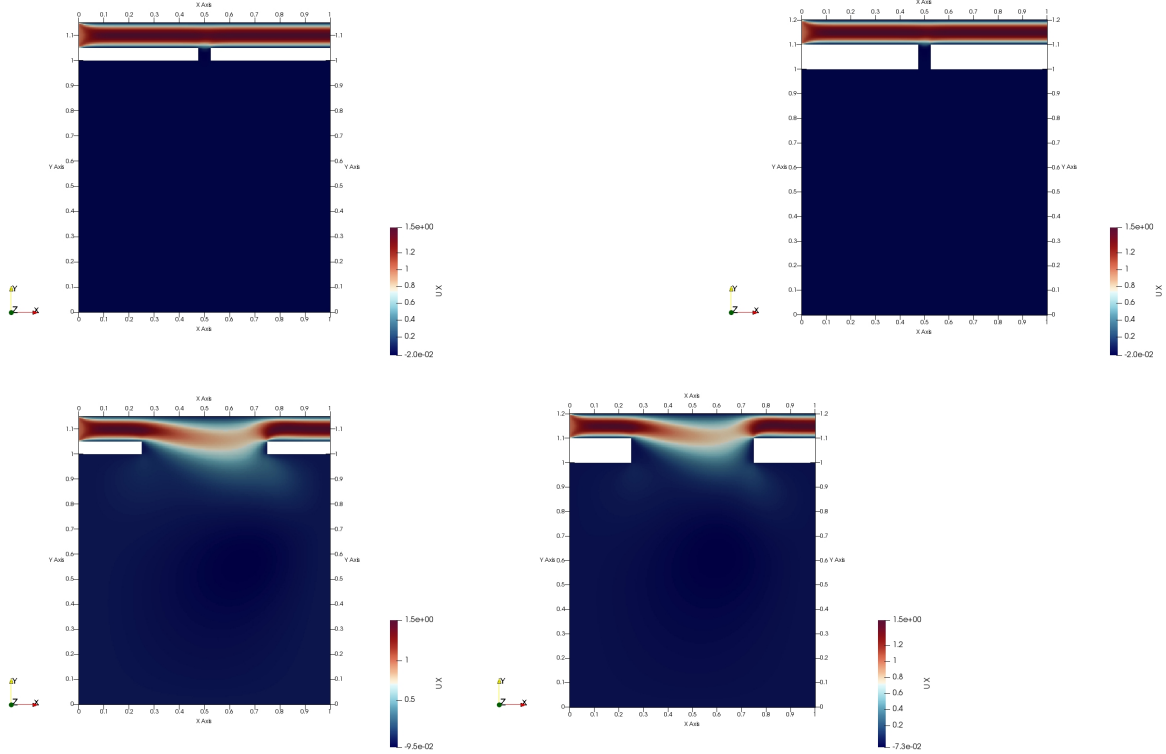
This is confirmed by the streamline plots. Note that there are between 1-3 transition vortices. At maximum, with the most neck-like window, there is a vortice the window opening, one in the window another in opening to the cavity. These three vortices connect the crossflow to the internal centralized vortex. When the window is broadened, these vortices all combine to form a single large transition vortice. Finally, note the center of the centralized vortice is very close to the center, and the crossflow bend is similarly symmetric, despite the flow directionality. This symmetry is probably due to the low Reynolds number of the flow.

## Re=200, Pressure



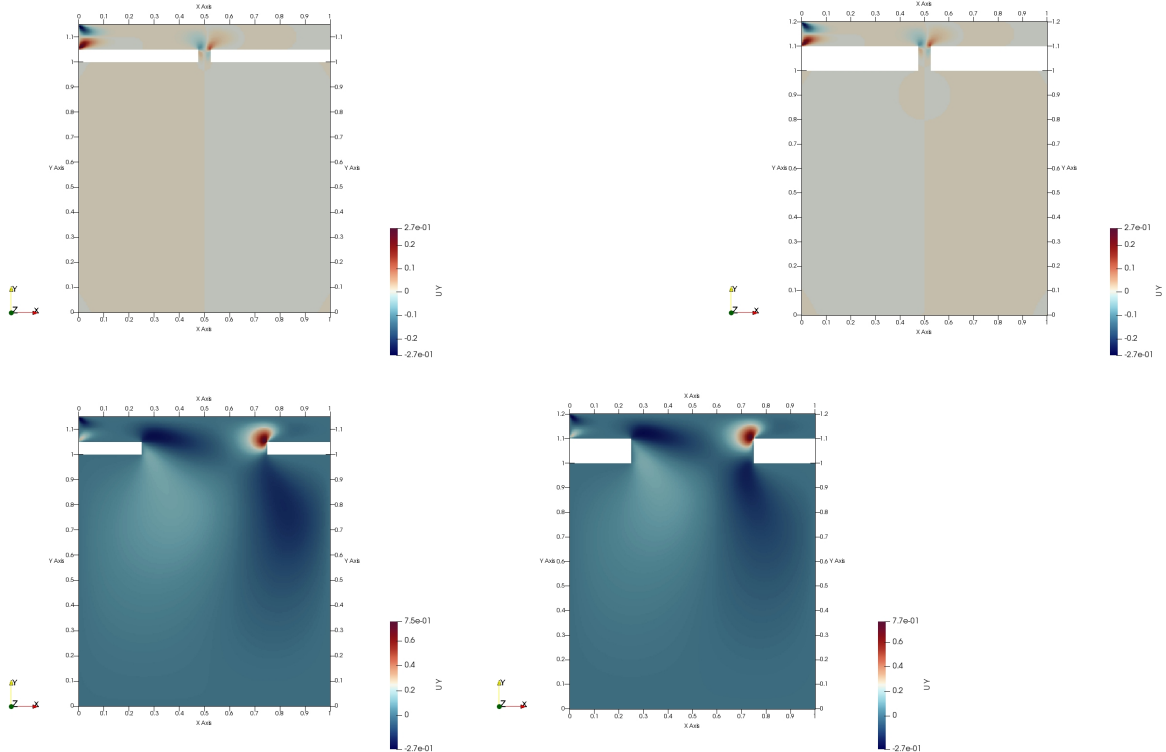
The pressure for Re=200 is very similar to that of Re=10 - the cavity acts like a simple pressure sink.

## Re=200, X-velocity



The only major difference is the asymmetry, which is probably due to the Reynolds number. Note that these solutions are also stable, and have been checked by flow visualization over time.

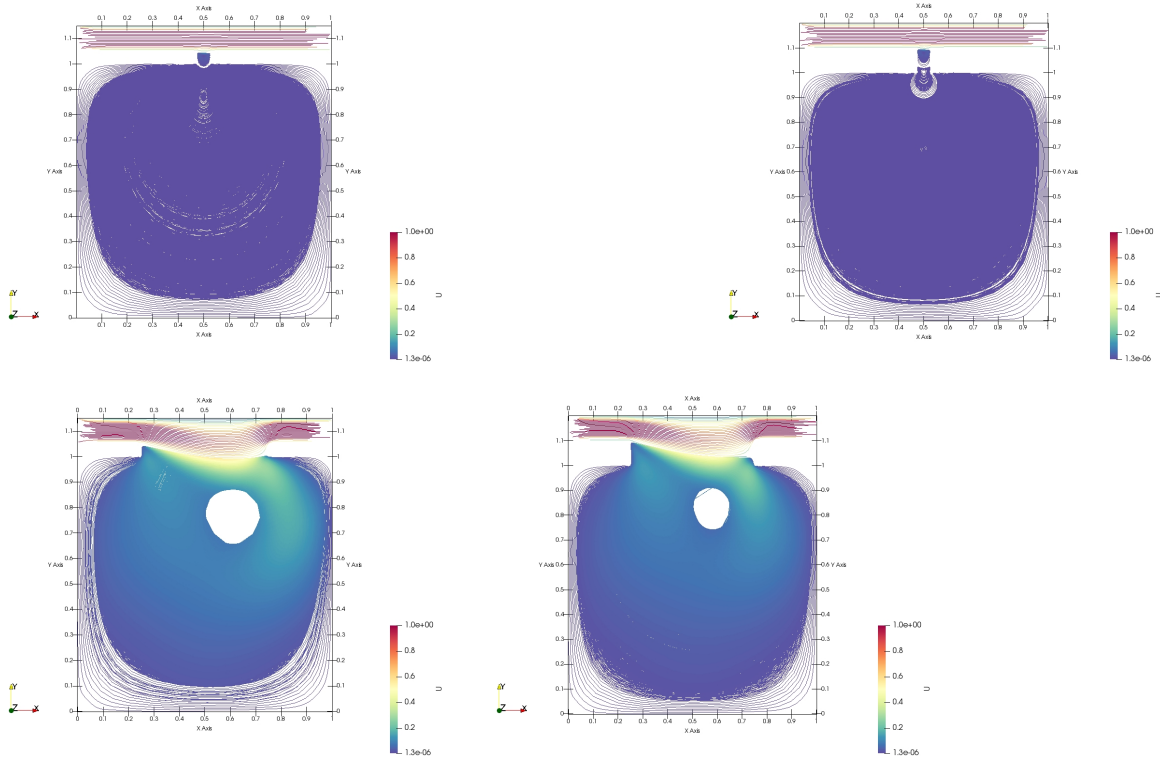
### Re=200, Y-velocity



Note that in addition to the asymmetry (same as seen in the x-velocity plots), there is an additional hydraulic jump right at the upper-right window corner, as the flow resumes high speed.

We will return to this in the high Reynolds section, as with increasing Re, this sort of jump can cause additional effects. We can also see the prominent third transition vortice clearly in the top-right plot.

## Re=200, Streamlines



Note the prominent third transition vortice. Otherwise, everything is as expected from Re=10 flow, except for the asymmetry.

## 5.5. Vortice Positions

Convergence can easily be seen by looking at the centralized vortex position for both meshes, by differing geometry.

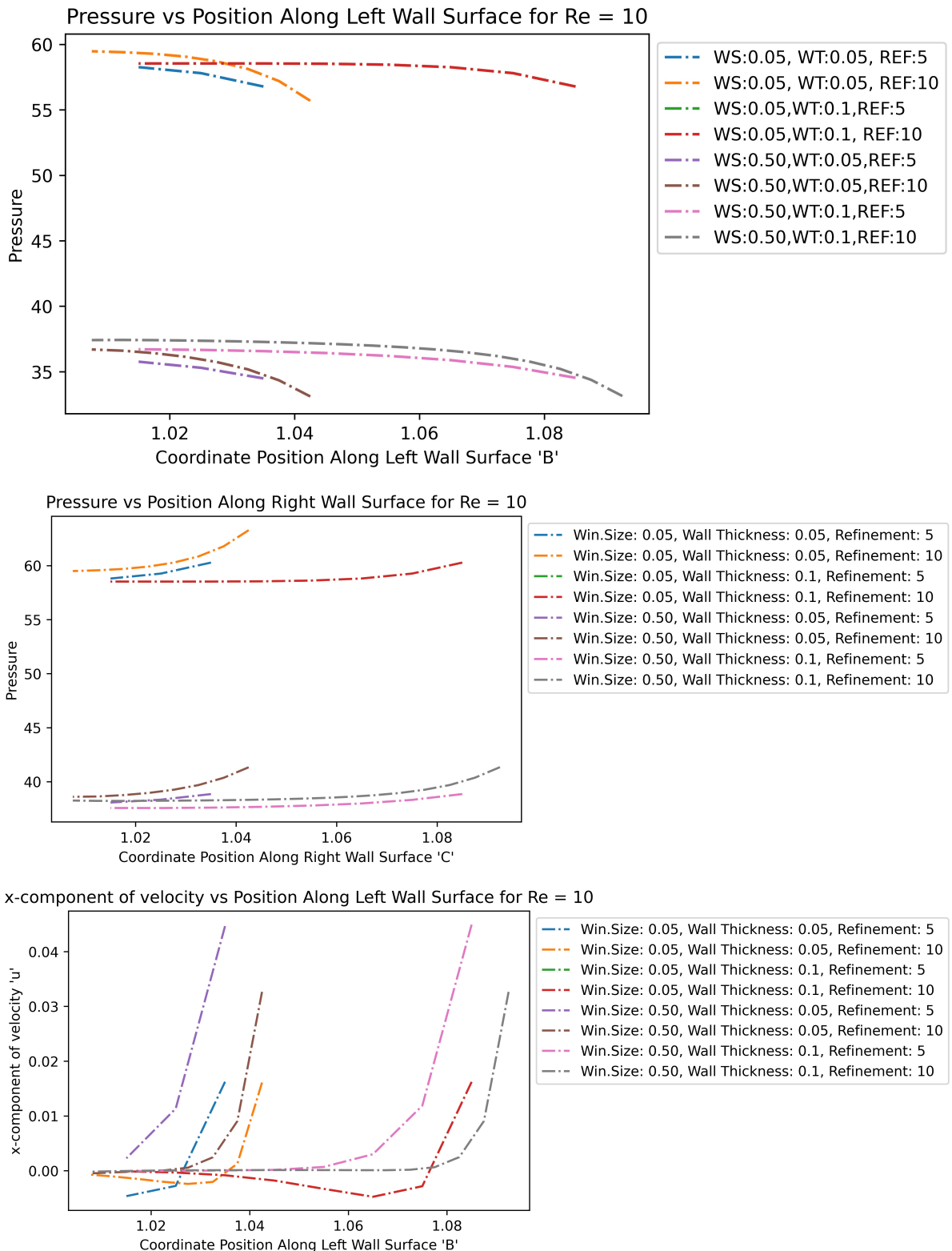
<b>meshfactor</b>	<b>Reynolds</b>	<b>window.a.</b>	<b>wall.w.</b>	<b>Vortex.Center.Location.along.Y</b>
5	10	0.05	0.05	0.8350
10	10	0.05	0.05	0.8525
5	10	0.05	0.10	0.9650
10	10	0.05	0.10	0.9650
5	10	0.50	0.05	0.5650
10	10	0.50	0.05	0.5725
5	10	0.50	0.10	0.6050
10	10	0.50	0.10	0.6075
5	50	0.05	0.05	0.8350
10	50	0.05	0.05	0.8525
5	50	0.05	0.10	0.9650
10	50	0.05	0.10	0.6075
5	50	0.50	0.05	0.6550
10	50	0.50	0.05	0.6625
5	50	0.50	0.10	0.6850
10	50	0.50	0.10	0.6875
5	200	0.05	0.05	0.8550
10	200	0.05	0.05	0.8675
5	200	0.05	0.10	0.9750
10	200	0.05	0.10	0.6875
5	200	0.50	0.05	0.7650
10	200	0.50	0.05	0.7725
5	200	0.50	0.10	0.8250
10	200	0.50	0.10	0.8325

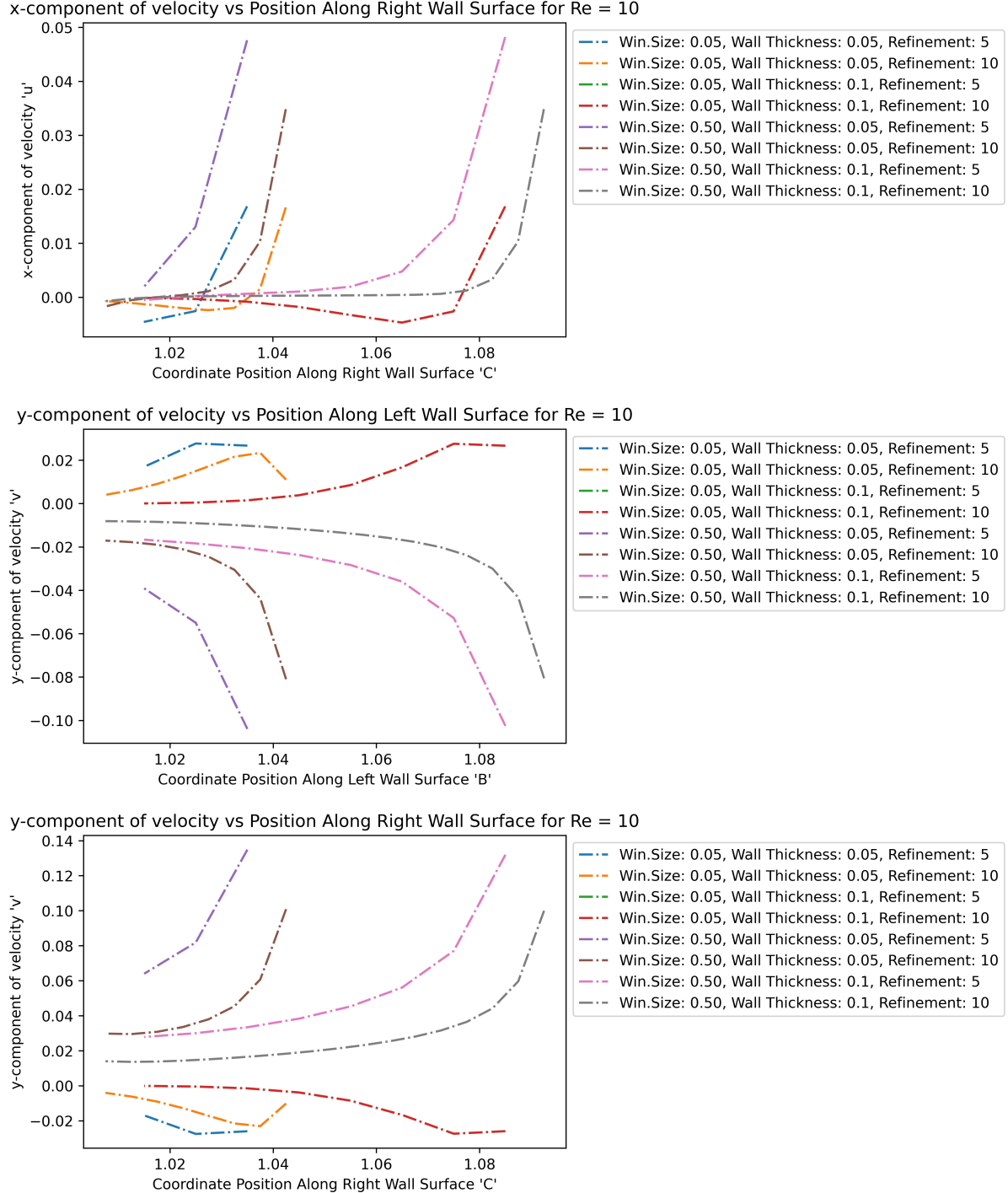
Table 4:

### 5.6. Window Wall Solution Profiles

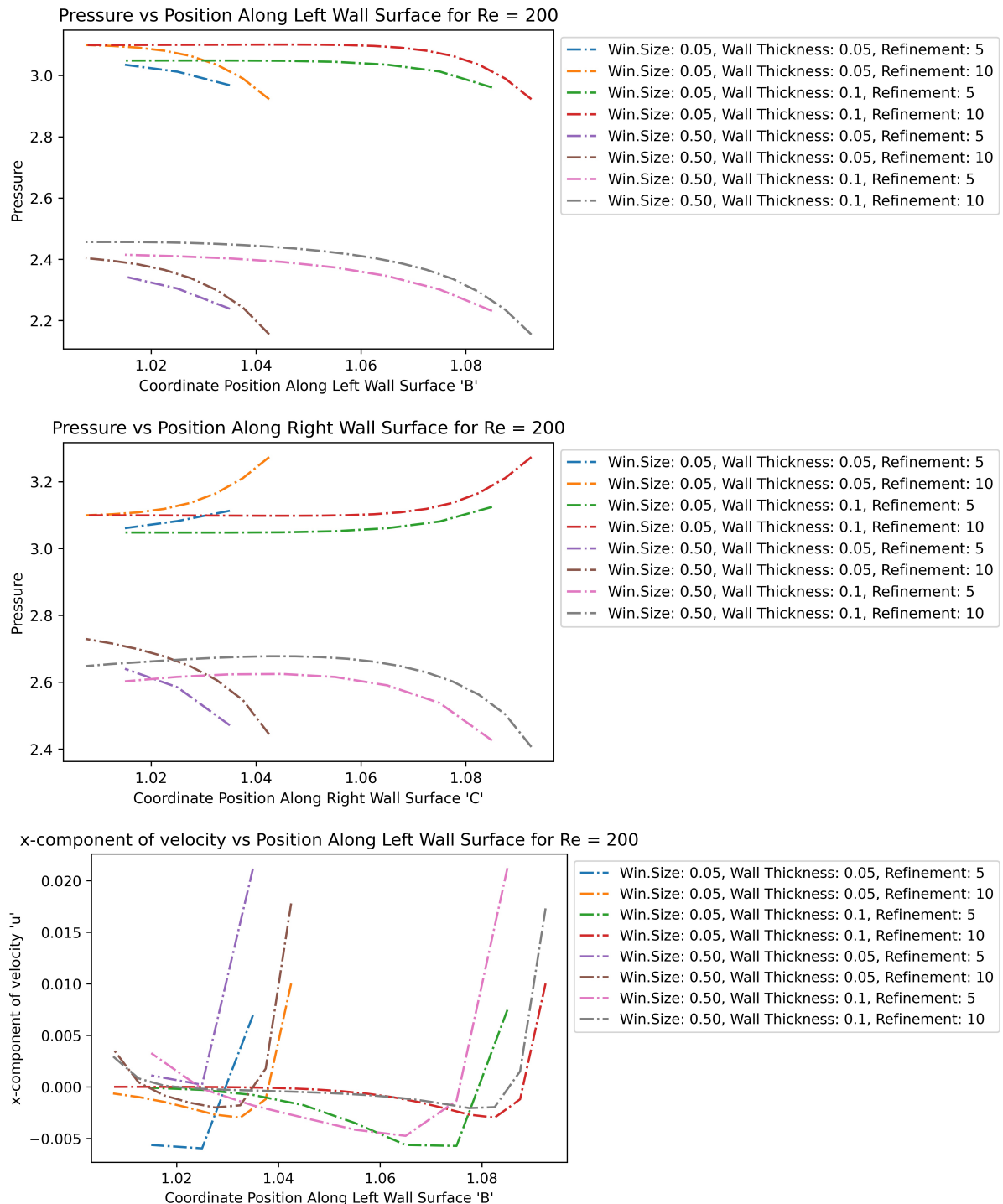
Now consider the profiles along the left and right window walls; the vertical segments along the inside of the window.

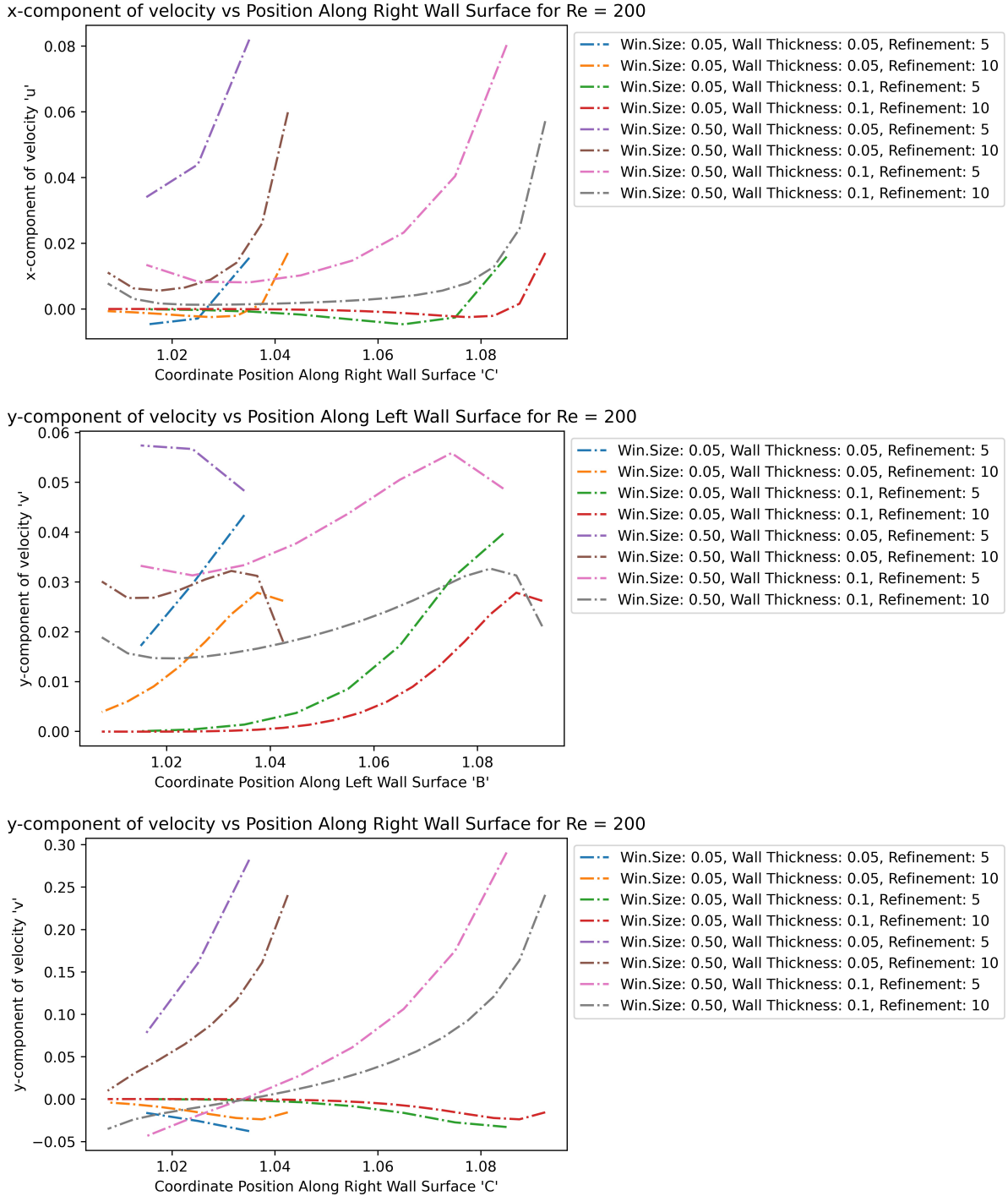
**Re=10**





**Re=200**

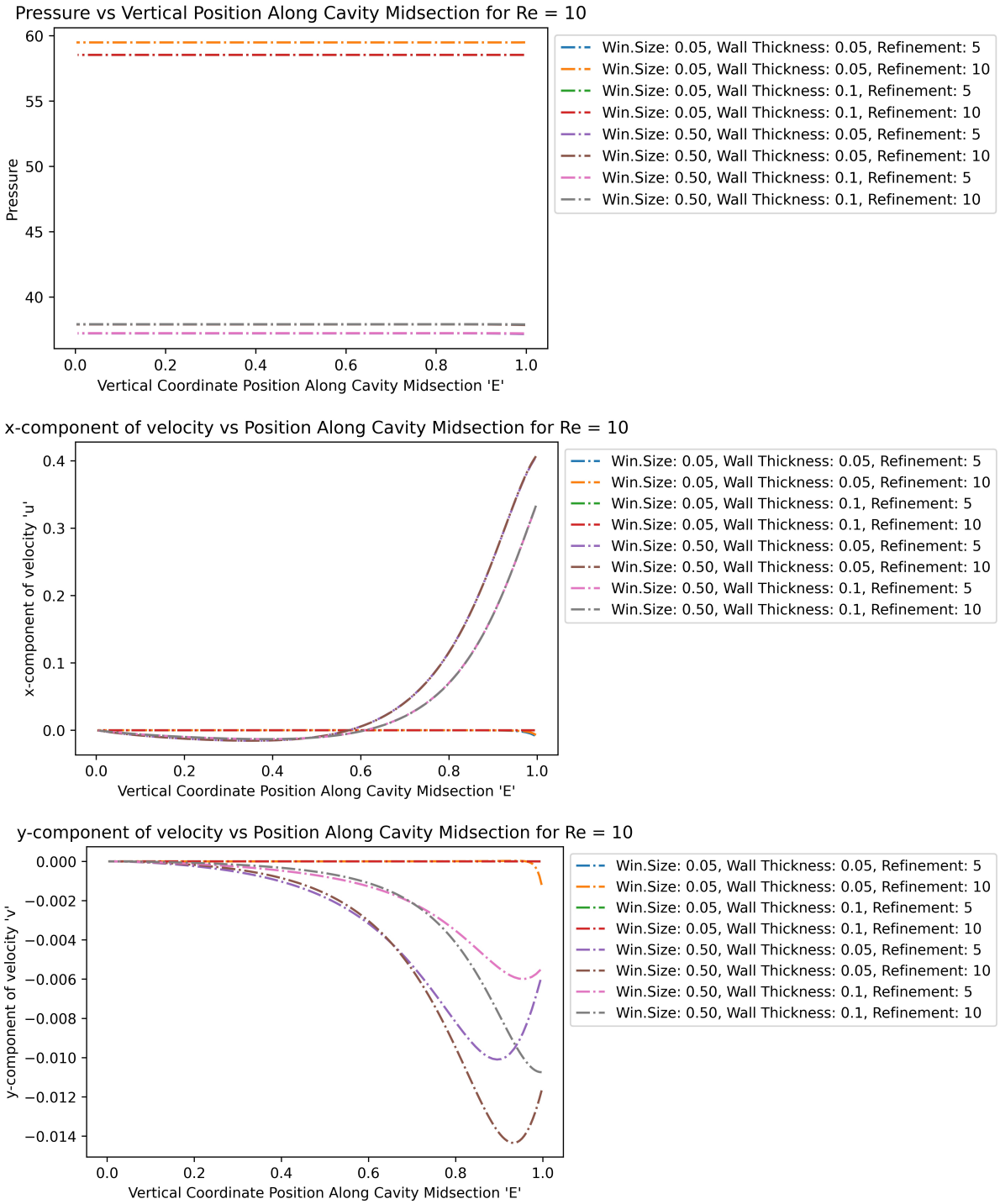




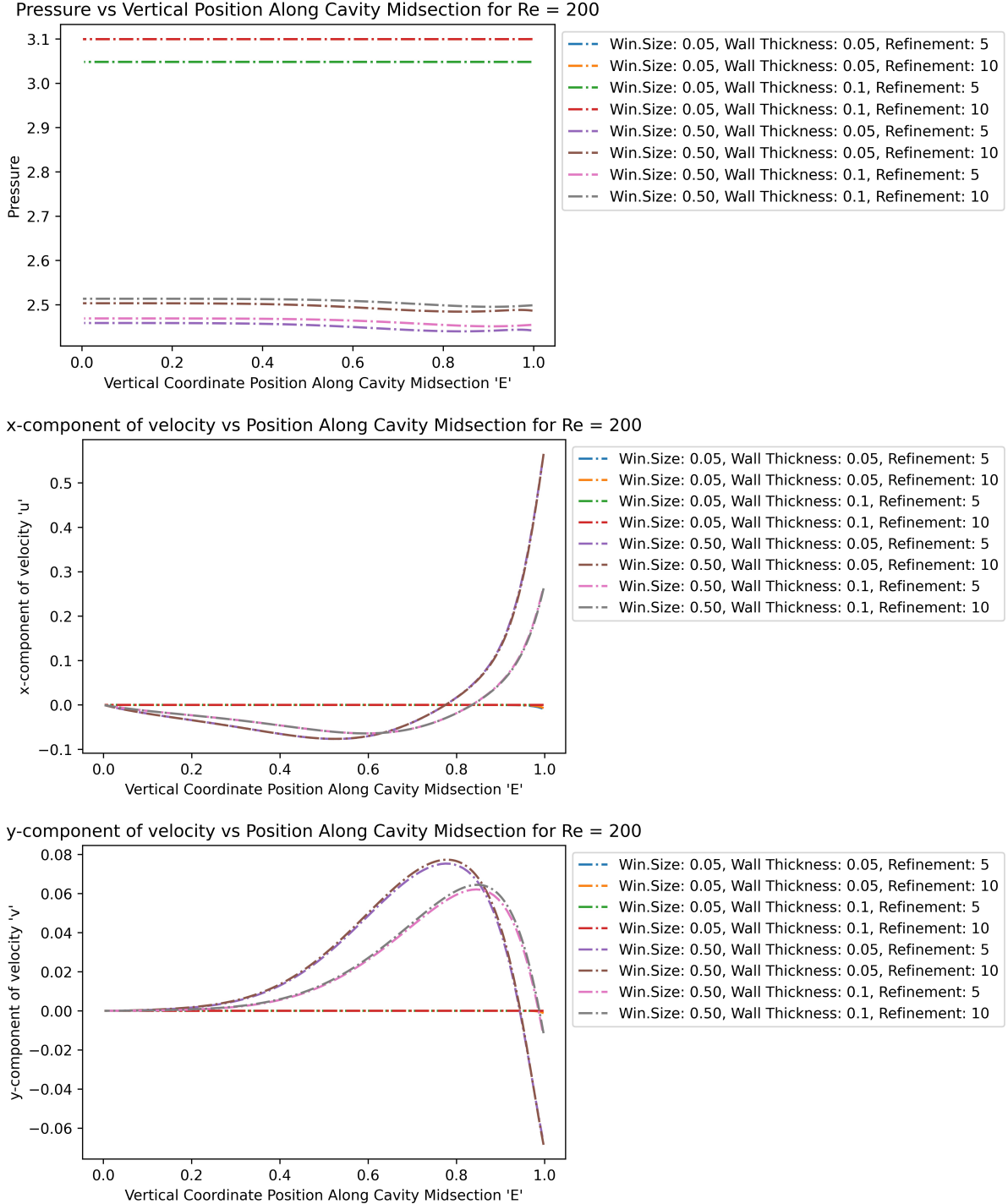
### 5.7. Cavity Midline Solution Profile

Now consider the profiles along the vertical midline down the cavity; from the middle of the window down to the back of the cavity.

**Re=10**



**Re=200**



## 6. High Reynolds Number Part 1

Although low-speed Reynolds number flow is beneficial for primary flow analysis, the flow in such a scenario would not prove catastrophic. Storms, be it hurricanes or tornados, contain flow of a high Reynolds number as is proportional to the velocity. In this section the flow behavior within a cavity of uniform wall thickness and window width will be analyzed with a high Reynolds number freestream flow outside of the cavity.

Note again all values are nondimensionalized - all lengths are in terms of  $L$ , the cavity length, all speeds in terms of  $U$ , the initial flow speed, and all times in terms of  $\frac{L}{U}$ .

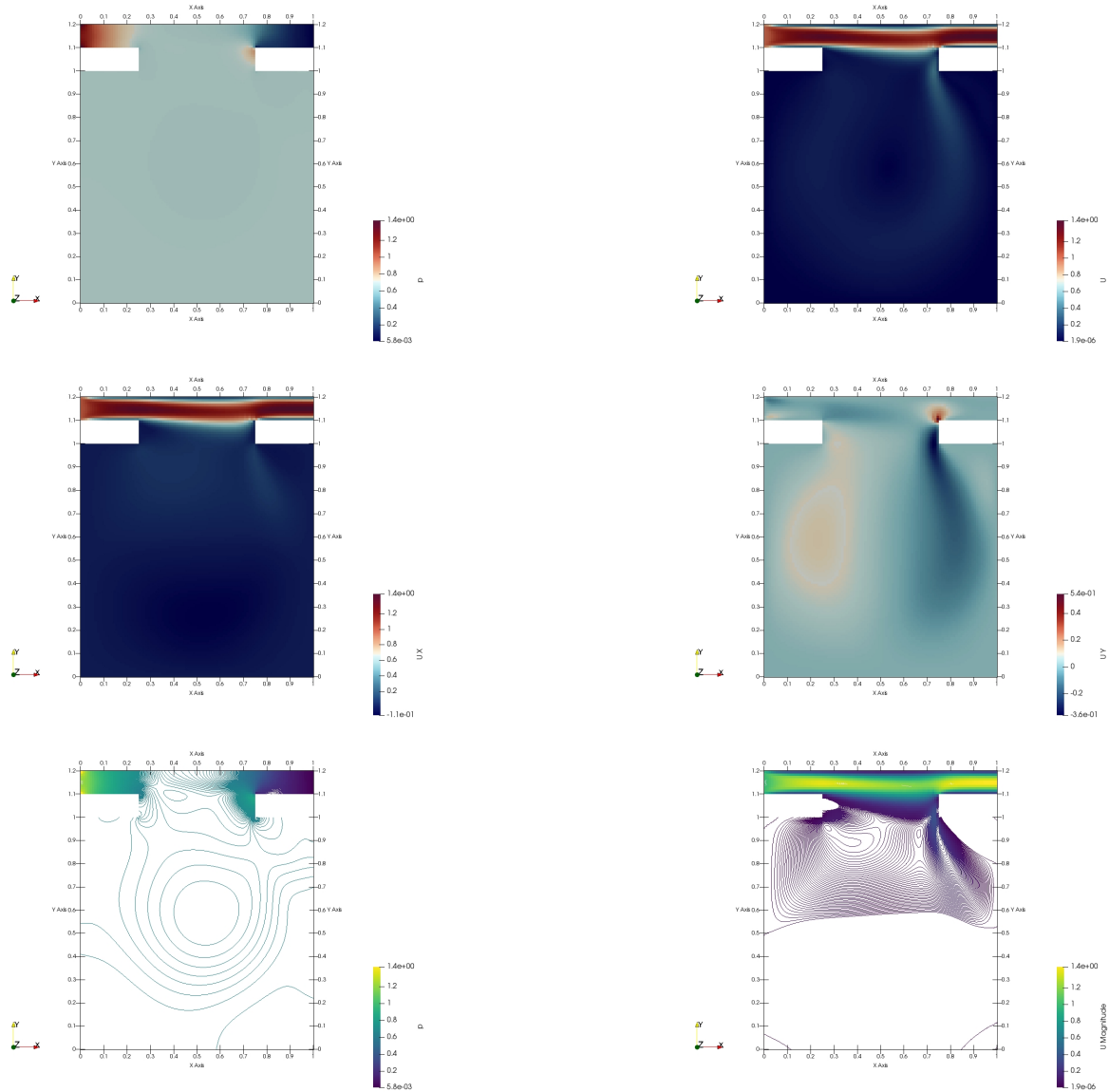
The pressure is in terms of  $\frac{p}{\rho U^2}$ .

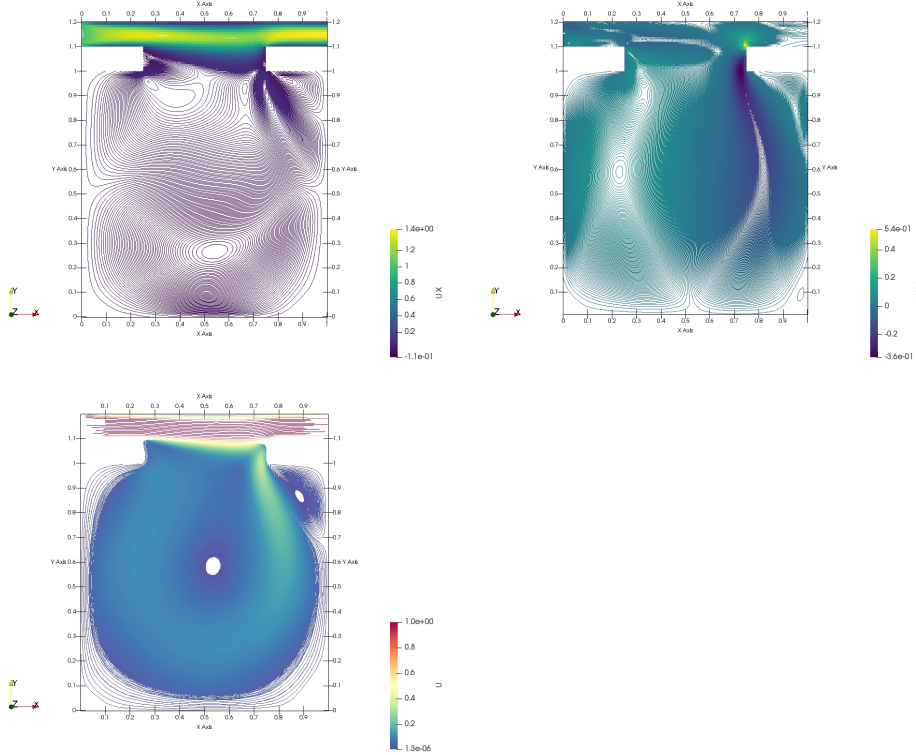
## 6.8. General Solution Form

Given the results from the Low Reynolds simulations, we will now consider only a window width of 0.5 and a wall thickness of 0.1. Images only for the refined mesh will be shown, for brevity.

Plots will be shown in the following order: P, U, UX, UY, P-contour, U-contour, UX-contour, UY-contour, Streamlines for T=60.

**Re=1000**

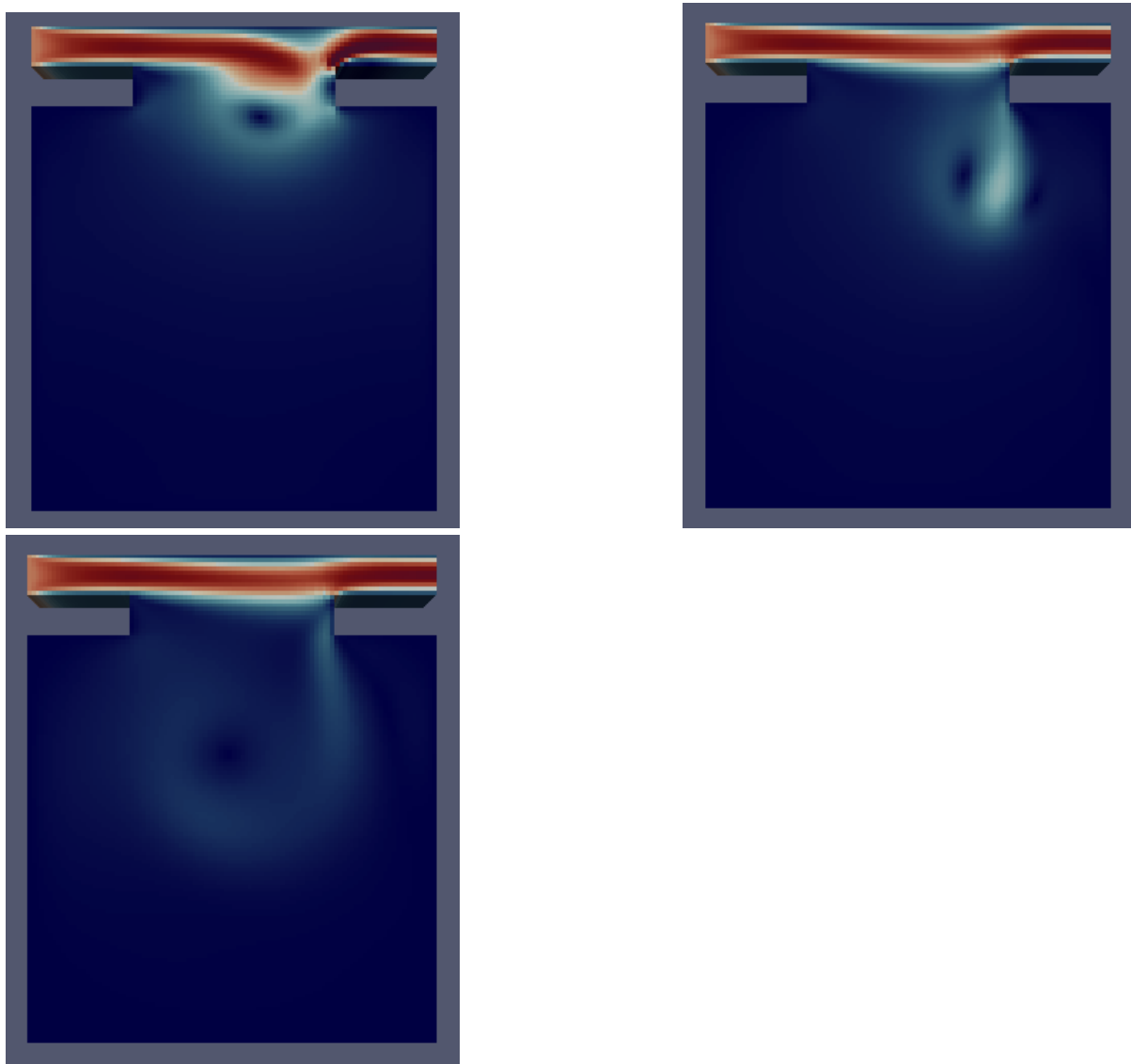




There is obvious vortex shedding at the right wall; one can see a tail extending into the cavity in nearly all the plots. Otherwise, this is quite similar to the low-Reynolds flow!

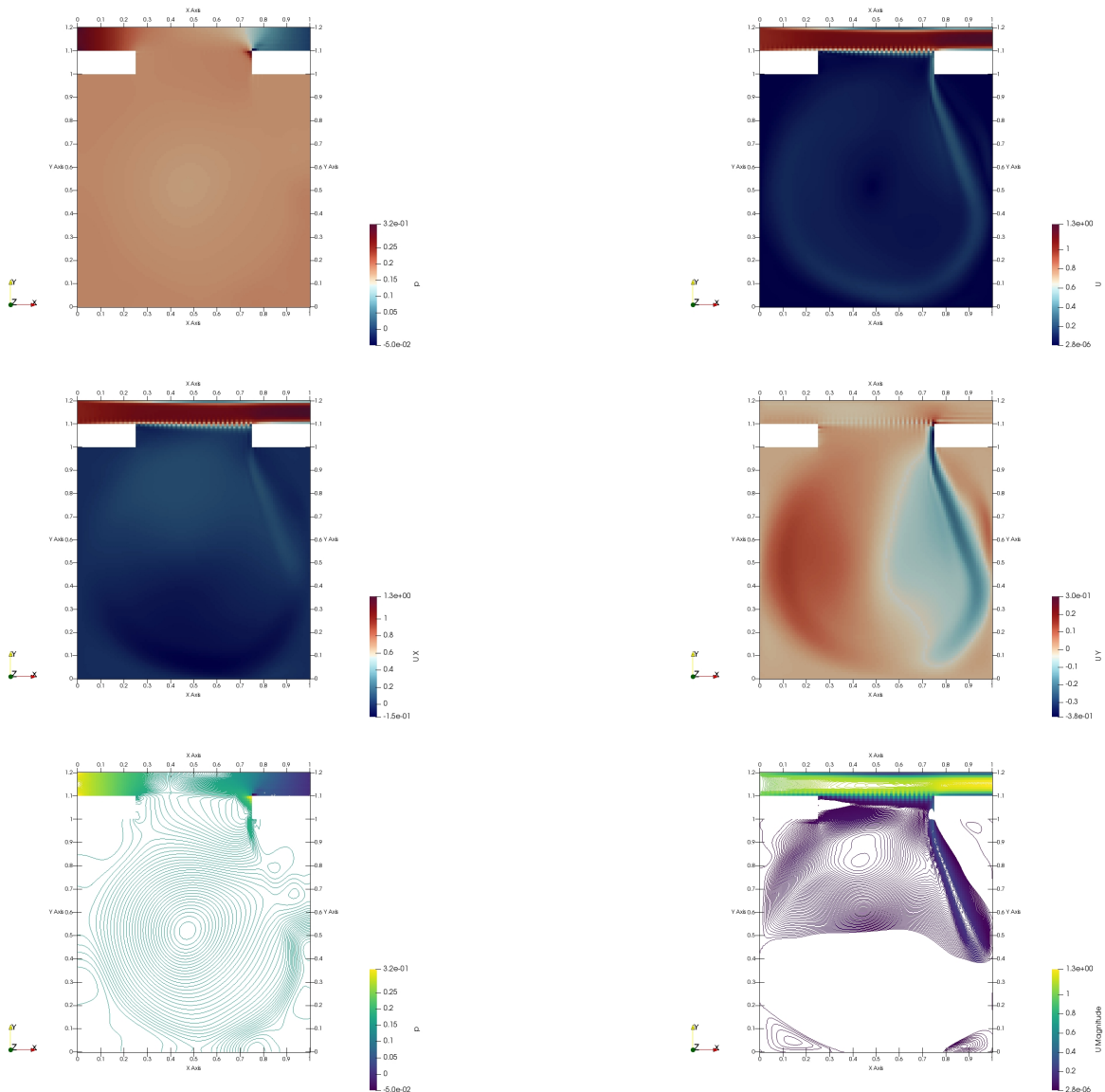
There is again a centralized vortice, an asymmetrical bend in the crossflow, and the hydraulic jump at the top of the right wall. The only difference is the tail, possibly a von Karman vortex street. To confirm that this is an unsteady flow, we look at the flow evolution over time.

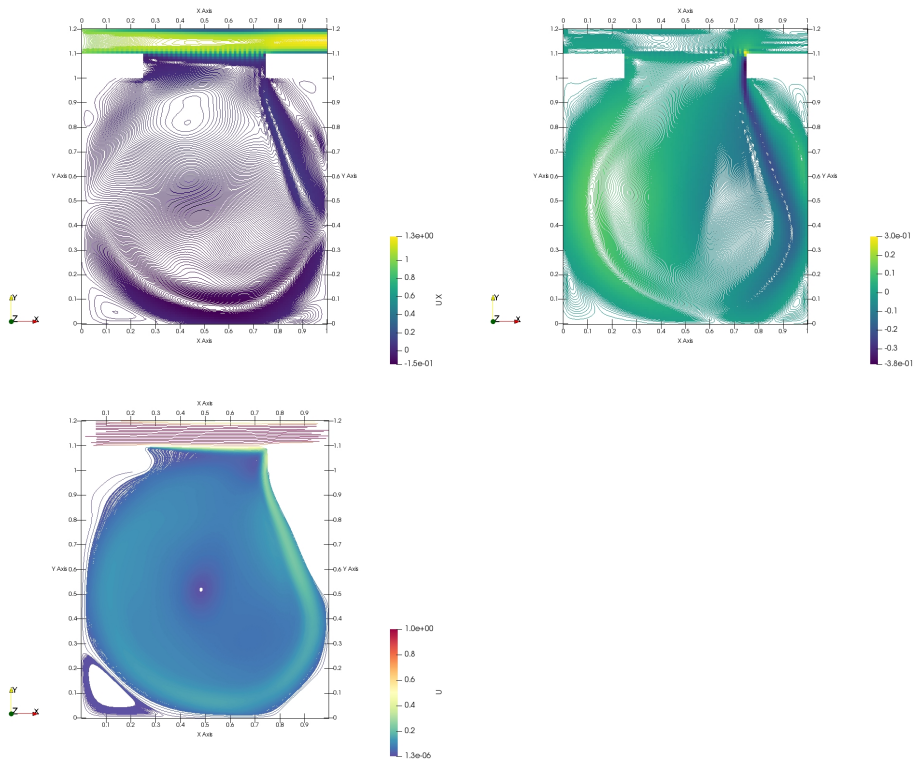
**Re=1000, U at T=1,2,6**



Clearly the flow is steady at large scales! So the vortex tail may not actually be a vortex street, since the unsteadiness is only at small scales. So  $\text{Re}=1000$  is the above the lower-limit for the critical Reynolds number for large-scale flow, and below the critical Reynolds for small-scale flow. The overall critical Reynolds must then be between  $\text{Re}=200$  and 1000.

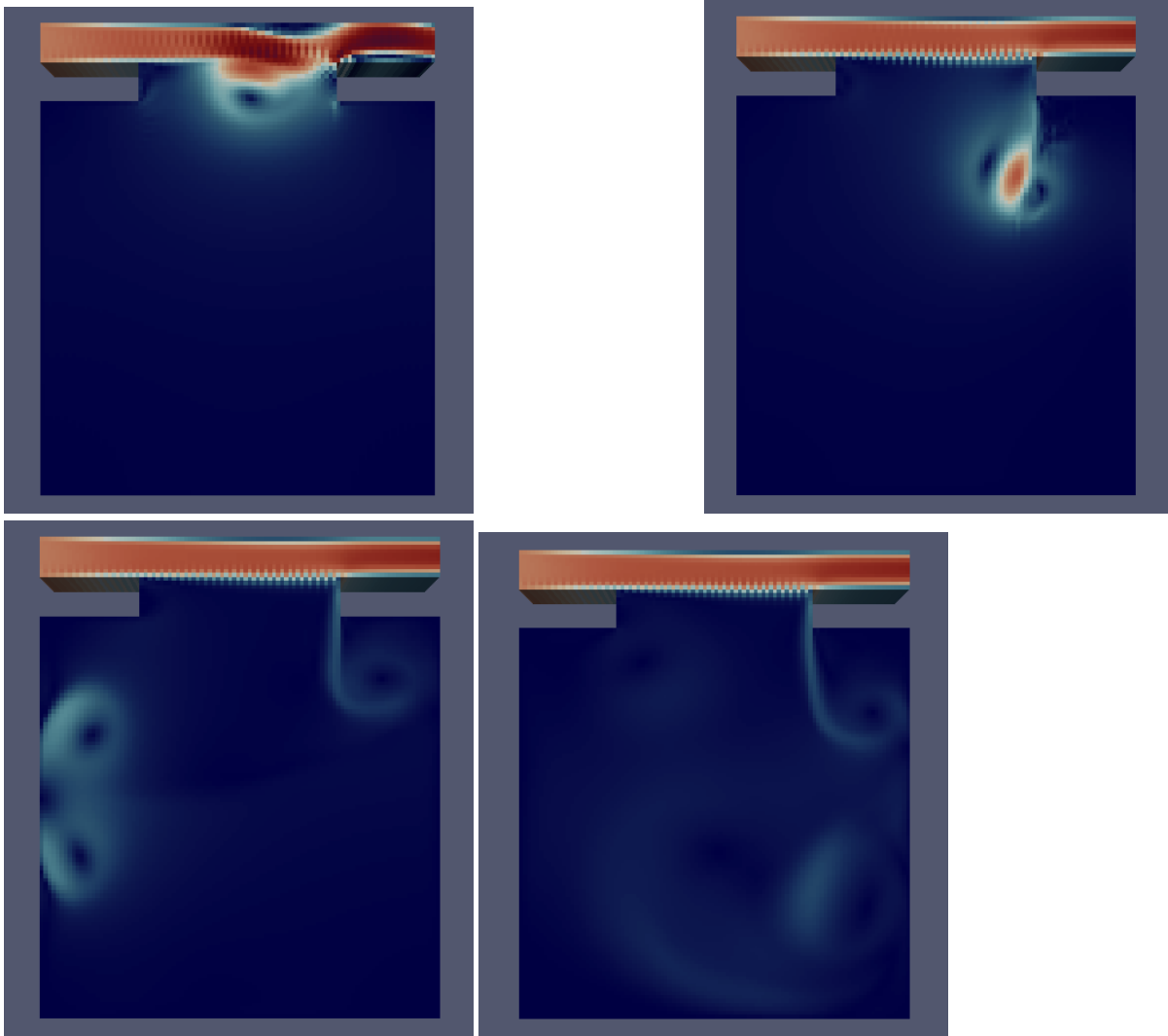
**Re=1000**





A much more well-defined vortex street can be seen here, and the only differences are really a more asymmetric flow with a stronger vortex street. This street can now be called such, since it does shed large-scale vortices, as seen in the following images over time. An important note: the vortex street originates from the hydraulic jump and propagates backwards, much like disturbances and sometimes turbulence can be seen behind a tidal bore or river rapids.

**Re=10000, U at T=1,2,6,30**



### 6.9. Vortice Positions

Convergence can again easily be seen by looking at the centralized vortex position for both meshes, by differing geometry.

<b>meshfactor</b>	<b>Reynolds</b>	<b>window.a.</b>	<b>wall.w.</b>	<b>Vortex.Center.Location.along.Y</b>
3	1000	0.5	1	0.691667
5	1000	50.0	1	0.705000
3	10000	0.5	1	0.641667
5	10000	50.0	1	0.595000

Table 5:

### 6.10. Strouhal Number and Vortex Shedding

The strouhal number is a dimensionless value that describes the behavior of flow oscillation. A very low Strouhal number denotes very few perturbations in the flow, whereas a very high Strouhal number denotes viscous behavior - while a moderate Strouhal number indicates vortex shedding.

We will now look at the frequency of the vortex shedding that occurs at the right window wall. In non-dimensional form (in terms of  $L/U$ ), this is the Strouhal number. Two probes are placed 0.025 to the left and right of the right vertical wall, 0.05 below the lower

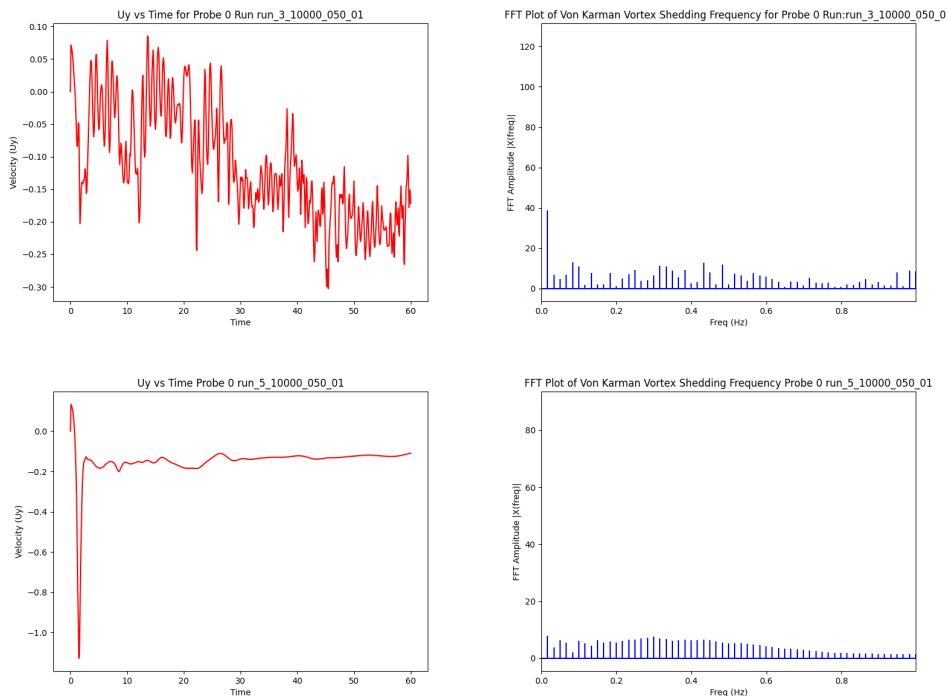
edge. We will denote the left probe as probe 0, and the right probe as probe 1. Coarse meshes will be shown along with their refinements.

### Fast Fourier Transform (over all time)

From the images shown earlier, clearly there is no vortex shedding for the  $Re=1000$  case, and it seems to stabilize quickly, so one might assume that the flow is steady.

Below we have only treated the  $Re=10000$  case, since the  $Re=1000$  case does not produce useful filtered output (which might seem to corroborate the above.)

#### Re=10000, Probe 0



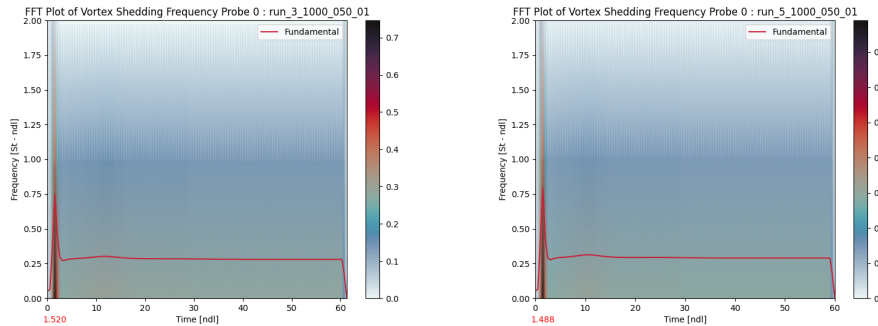
#### Re=10000, Probe 1



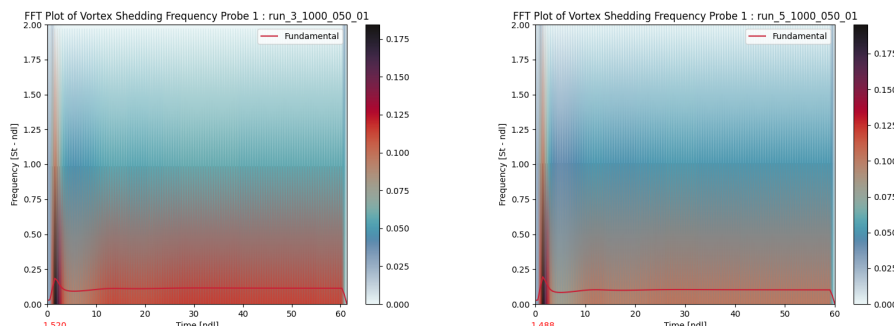
Note that the meshFactor of 3 fails to capture solution behavior (see the added oscillation).

### **Short Time Fourier Transform (spectrogram to see time evolution)**

#### **Re=1000, Probe 0**



#### **Re=1000, Probe 1**

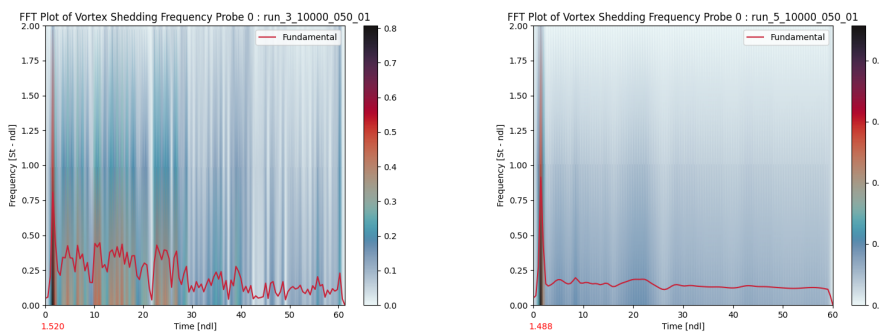


Interestingly, the  $\text{Re}=1000$  plot is not at 0 Strouhal number! So we can clearly see that the large-scale flow does not have any steady-state oscillation (which is what the previous FFT plots show), but the small-scales are unsteady, with a typical Strouhal number near 0.2, as seen in the later table.

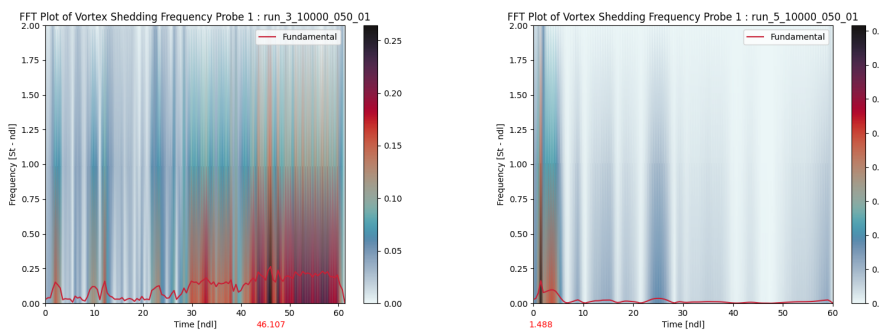
This is confirmed by the following:

For spheres in uniform flow in the Reynolds number range of  $8 \times 10^2 < \text{Re} < 2 \times 10^5$  there co-exist two values of the Strouhal number. The lower frequency is attributed to the large-scale instability of the wake, is independent of the Reynolds number  $\text{Re}$  and is approximately equal to 0.2. The higher-frequency Strouhal number is caused by small-scale instabilities from the separation of the shear layer.([Kim and Durbin 1988](#); [Sakamoto and Haniu 1990](#))

### **Re=10000, Probe 0**



### **Re=10000, Probe 1**



Continuing the former analysis, we see that the large scale instabilities are independent (since we get another Strouhal number for  $\text{Re}=10000$  near 0.2 later in the flow). On the other hand, the small-scale instabilities are more prominent here, in the form of disturbances to the transform. We do not capture the other Strouhal number due to placement of the probes; we are interested in the large scale flow, so the other Strouhal number is not relevant for this paper.

Note again that the meshFactor of 3 is insufficient to capture the solution.

### **Equilibrium Large-Scale Strouhal Values**

Note that transient Strouhal numbers exist for  $\text{Re}=1000$ , and there are also small-scale Strouhal numbers for  $\text{Re}=1000$ , but those are neither relevant nor easily retrievable for this study.

<b>meshfactor</b>	<b>Reynolds</b>	<b>ProbeNumber</b>	<b>Strouhal</b>
3	10000	0	0.116472
3	10000	1	0.166389
5	10000	0	0.316139
5	10000	1	0.149750

Table 6:

Note the stark difference between left and right frequencies - the higher one may be the second Strouhal number mentioned in the previously cited articles.

## 7. High Reynolds Number - Part 2

### 7.11. Window Wall Solution Profiles

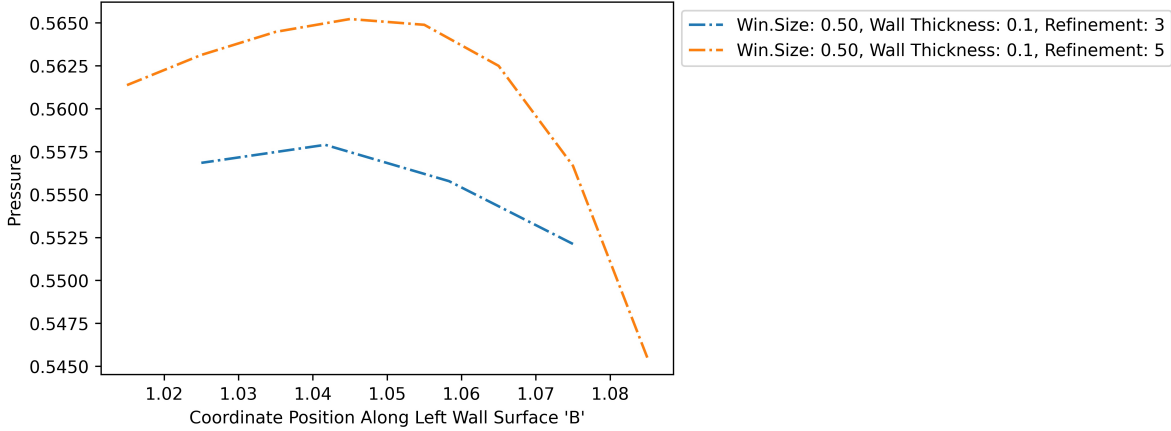
Now consider again the profiles along the left and right window walls; the vertical segments along the inside of the window.

This time we will consider the starting behavior of these profiles at high Re, in particular between T=1 and 2.

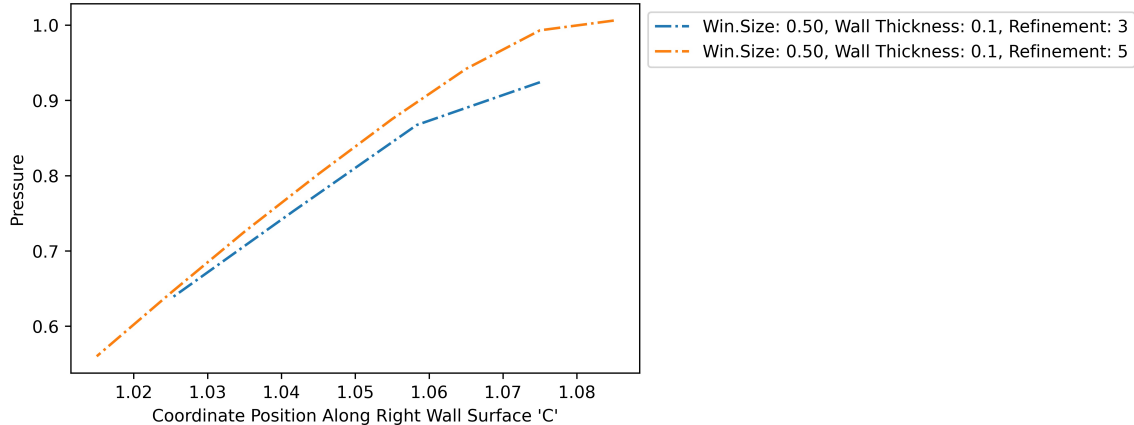
**T = 1.3 (unsteady startup)**

**Re=1000**

Pressure vs Position at t = 1.3 seconds Along Left Wall Surface for Re = 1000



Pressure vs Position at t = 1.3 seconds Along Right Wall Surface for Re = 1000

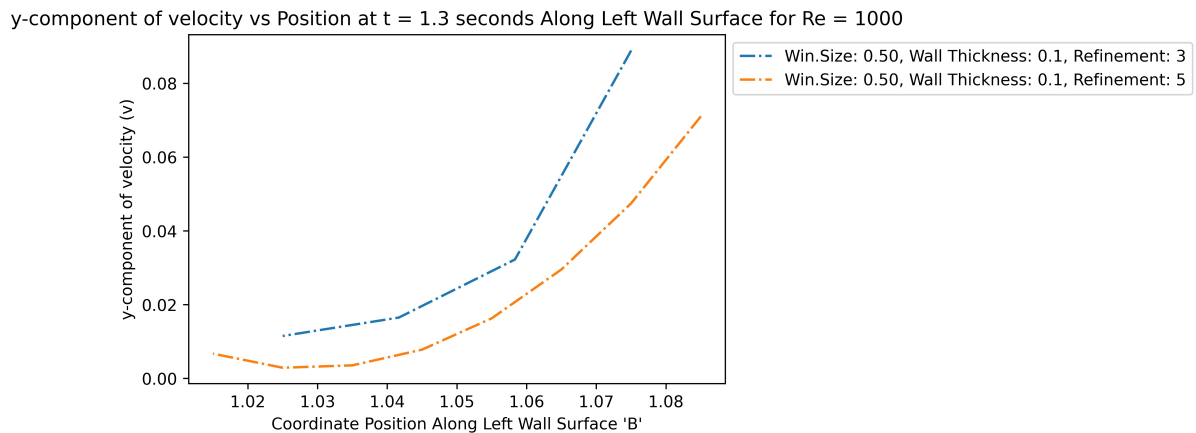
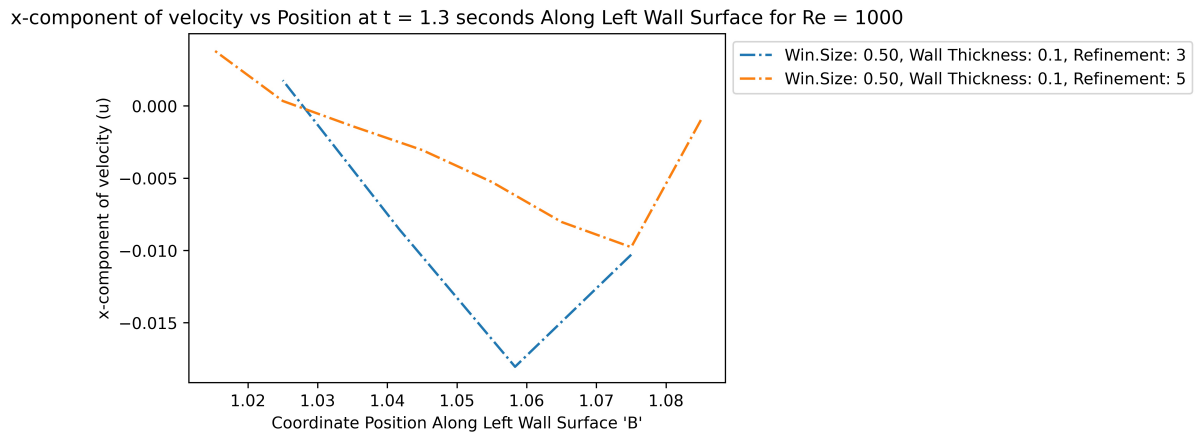


The pressure curves match the general images earlier; the only feature of note is the dip near 1.1, which is low pressure caused by rapidly accelerating corner flow.

The other dip at the cavity interior (near 1) is also due to the corner point; the lower velocity in the cavity compared to the crossflow causes the lower prominence of this dip.

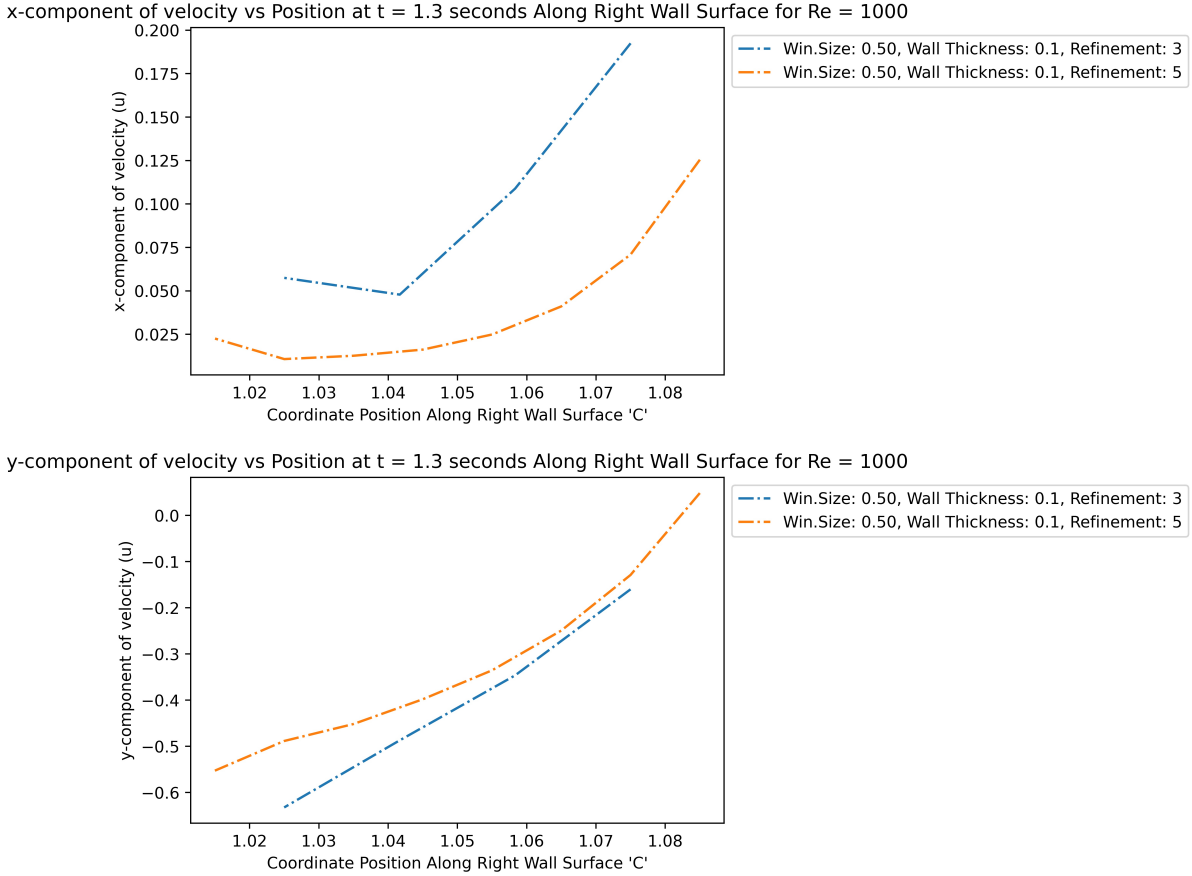
By contrast, the right wall has a vortex just leaving the wall, so the sample is basically from the vortex center to edge, and we can see that the low-pressure zone caused by vortice is  $0.5 \rho U^2$  lower than standard pressure.

### Left Velocity



Important to note here is the stagnation point near the lower corner (at  $y=1.3$ ). Both the X and Y velocities are 0 here. The flow above this point gets sucked back into the crossflow (as seen by the positive y-velocity and negative x-velocity) in a sort of recirculation, and the flow below this point remains in the cavity, moving up and right to join the part of the crossflow that enters the cavity.

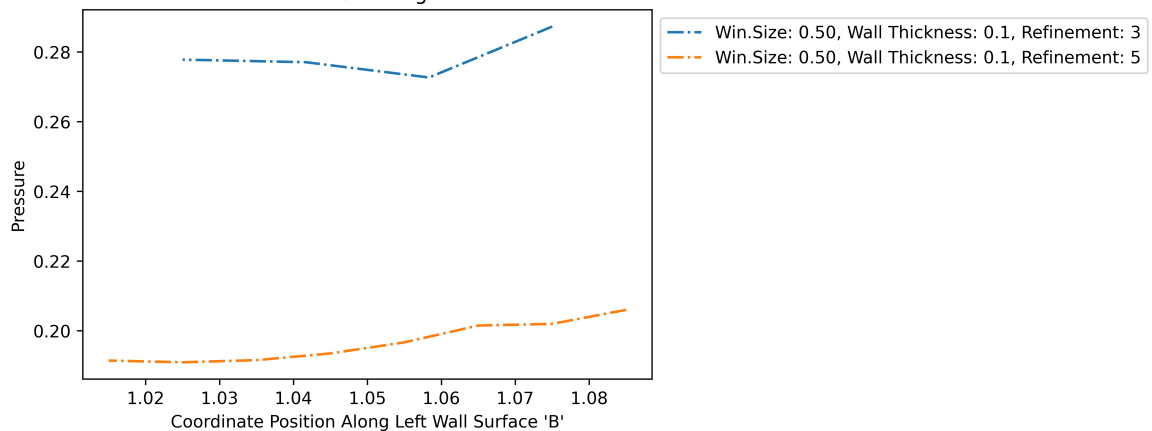
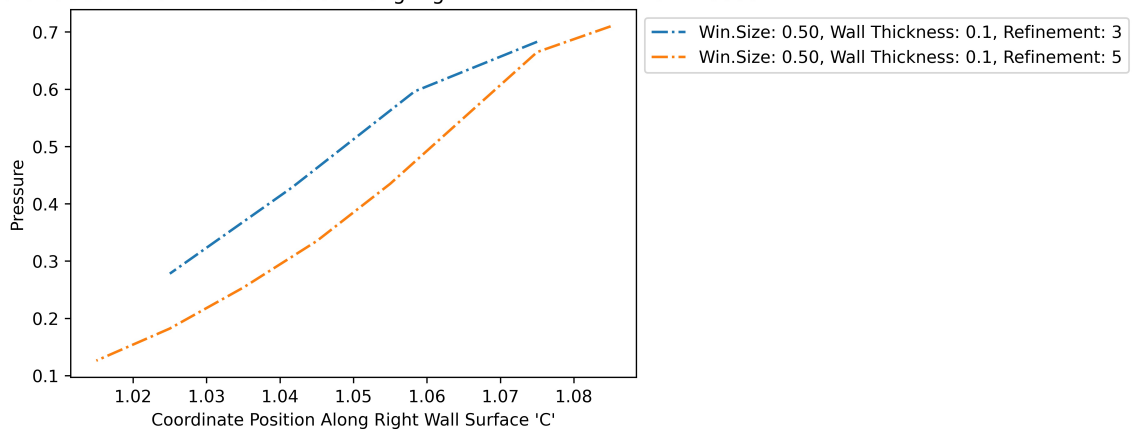
### Right Velocity



On the right wall, since we are sampling the edge of a vortice, the x-component is similar to  $1/4$  of a sinusoid (and this can be verified by noting from the earlier images that the vortice described here has a radius of approximately 0.1 (the wall width). The y-velocity is similarly sinusoidal, but has a strong negative velocity. Since we are almost sampling along the vortical radius, the velocity of the vortice wall should be roughly  $0.6 U$  (free-stream velocity), and the vortex center (or eye) is moving downward at  $0.6 U$ .

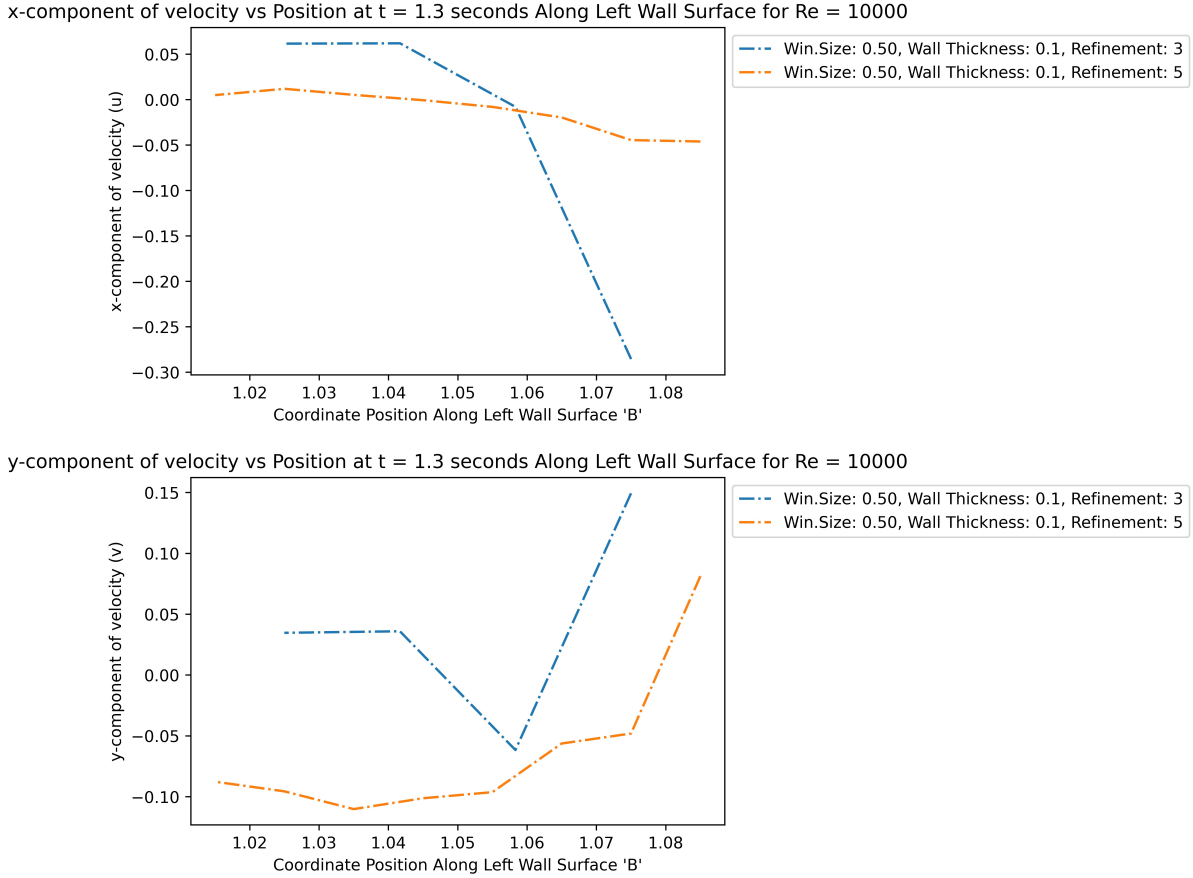
### **Re=10000**

Since from previous results, we have invalidated the refinement / meshFactor 3 for Re=10000 as being insufficient, that will not be considered for convergence in the following plots.

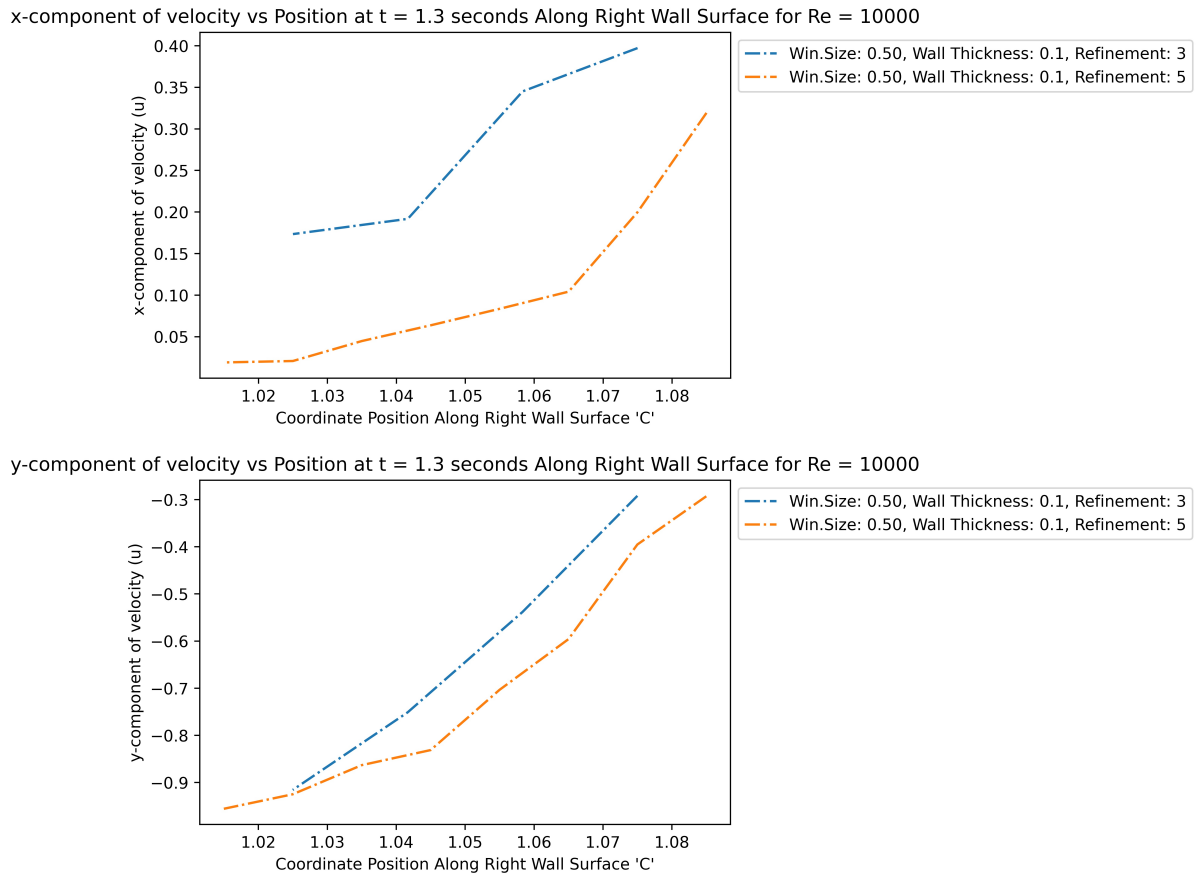
Pressure vs Position at  $t = 1.3$  seconds Along Left Wall Surface for  $Re = 10000$ Pressure vs Position at  $t = 1.3$  seconds Along Right Wall Surface for  $Re = 10000$ 

Just as before, the left wall has little to no pressure variation. Changing to  $Re=10000$  has replaced the upper-left corner flow with a high-pressure region, possibly a stagnation point, implying that any inflow now travels further past the corner before moving into the cavity. Again, the right wall approximates the pressure differential across the main vortice, which seems to be about  $0.65 \rho U^2$ . Note the sharp corner in the fine-refinement pressure; that is probably the vortice edge.

### Left Velocity



There is a really strong upward velocity with a negative x-component at the top-left corner, implying recirculation formation, which would correspond to the first transition vortice seen in low-Reynold flow. For the rest of the left wall, there is a small downward flow, possibly corresponding to the second transition vortice in low-Reynolds flow, again.



Again, from the images, this wall samples the main vortice. Looking at the X-velocity, and Y-velocity (stopping at the change in concavity), we see a difference in of about 0.3 and 0.6  $\rho U^2$ . So combining the speeds, the vortice speed (which will again be equal to rotation speed at edge) would approximately be about  $0.67 \rho U^2$  (using L2 magnitude). Notice that this matches with the pressure in these non-dimensional units (since  $U=1$ ), just like  $Re=1000$ , which is as expected.

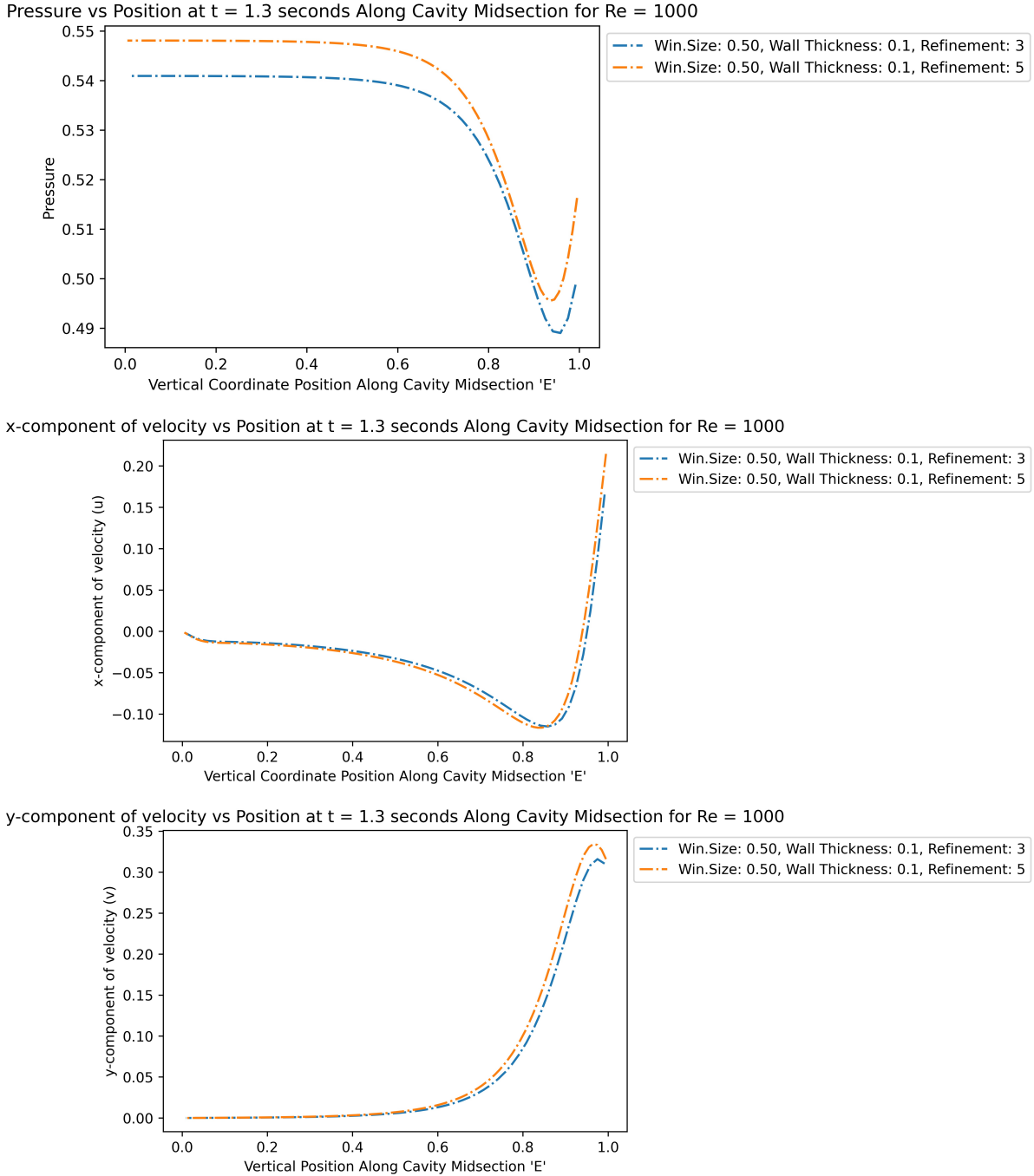
Interestingly, most of the flow-field, with the exception of the vortex shedding, is identical to the low-Reynolds, which might imply that portion of the flow causes the Strouhal number of 0.2.

## 7.12. Cavity Midline Solution Profile

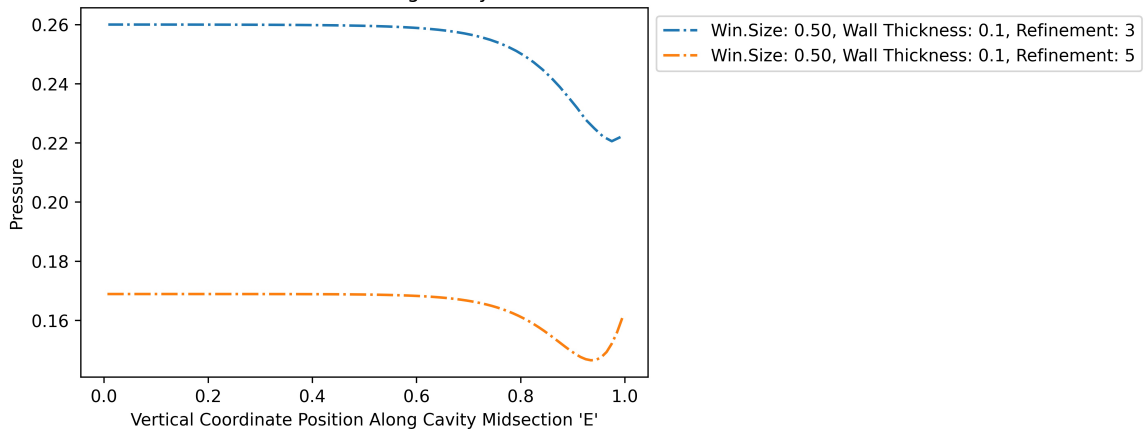
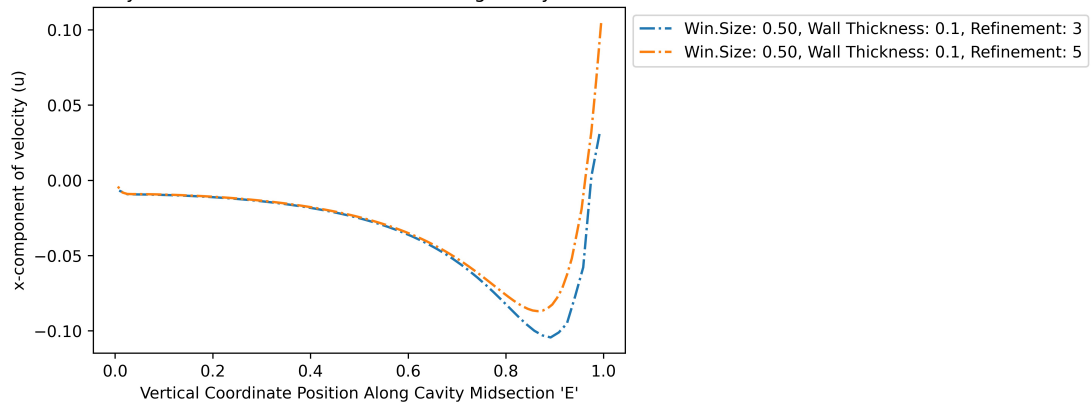
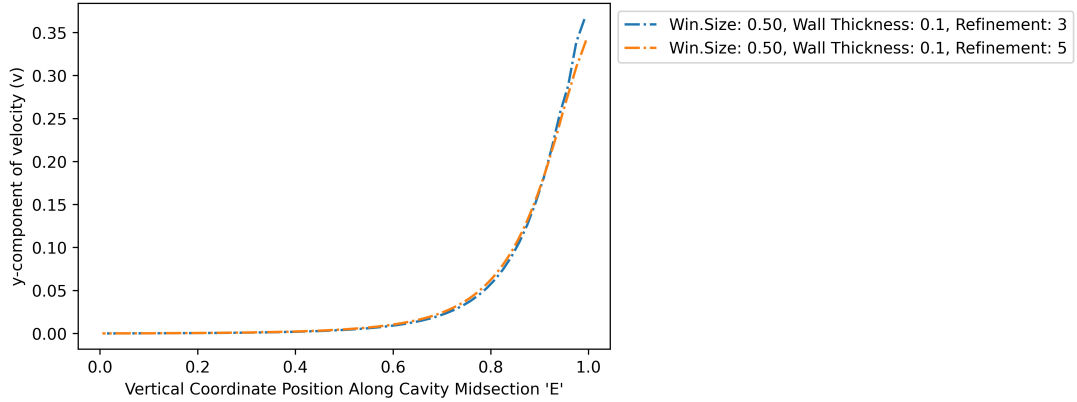
Now again consider the profiles along the vertical midline down the cavity; from the middle of the window down to the back of the cavity.

Similarly, we will only consider  $T=1.3$ .

**Re=1000**



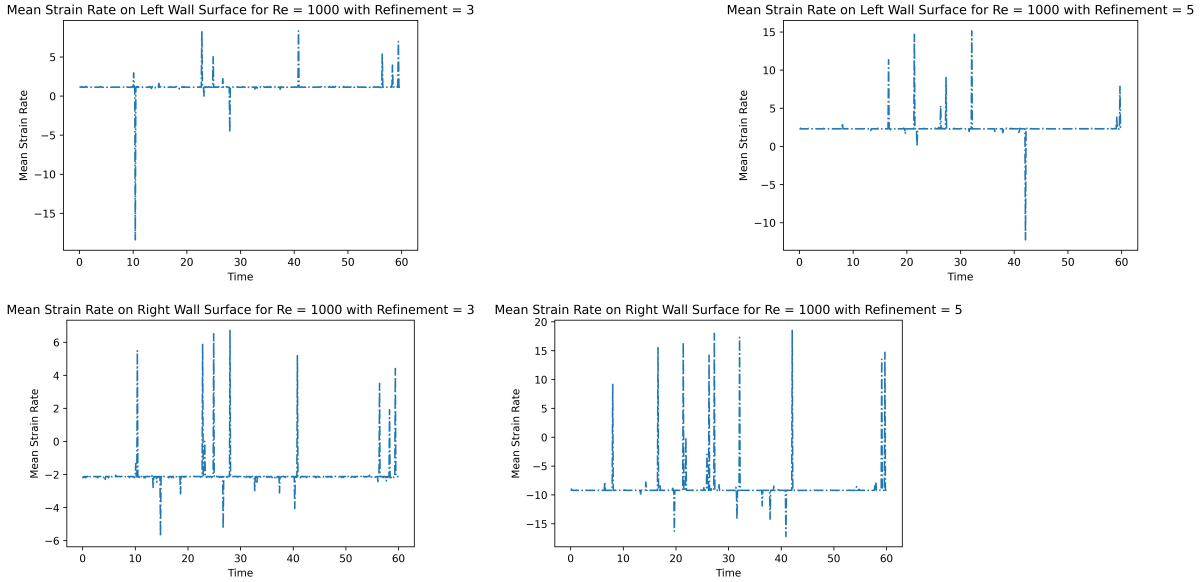
**Re=10000**

Pressure vs Position at  $t = 1.3$  seconds Along Cavity Midsection for  $Re = 10000$ x-component of velocity vs Position at  $t = 1.3$  seconds Along Cavity Midsection for  $Re = 10000$ y-component of velocity vs Position at  $t = 1.3$  seconds Along Cavity Midsection for  $Re = 10000$ 

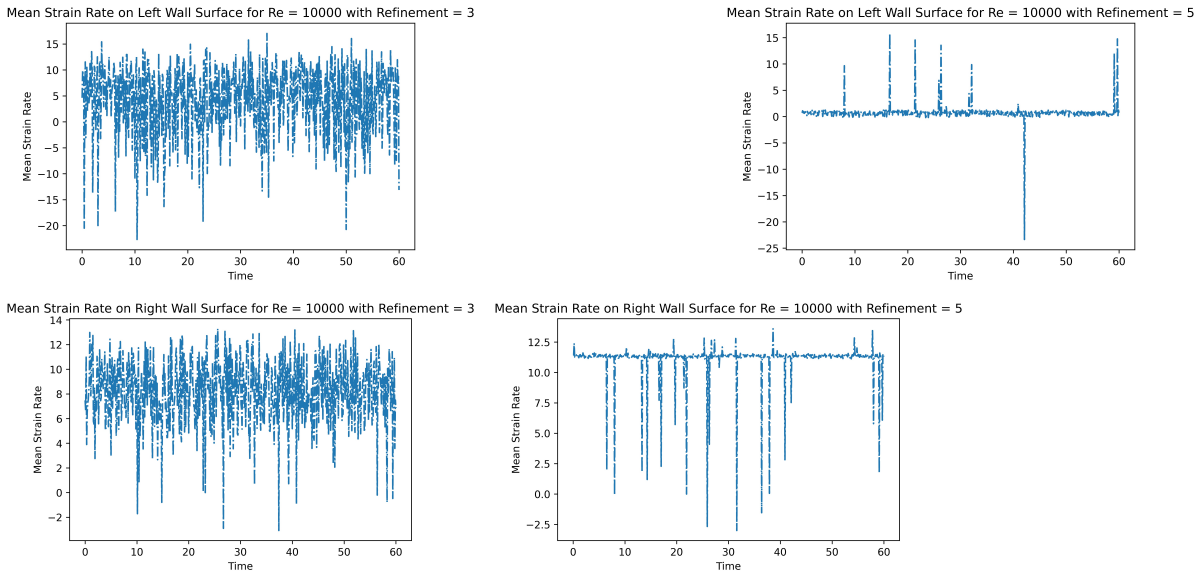
## Mean Strain Rate over Time

To confirm that the maximum strain rate does occur at  $T=1.3$ , we plot the mean strain rate over time, for the left and right vertical window walls.

**Re=1000**



**Re=10000**



Unfortunately, these results do not match  $T=1.3$  as maximum. Noting that the refinement or meshFactor 3 still fails for  $Re=10000$  in a manner similar to the previous plots, we can probably rule out code errors. The possible other issues might be a lack of sufficient refinement, since there does not seem to be uniform convergence - the spikes near  $T=60$  are similar, but other regions have sign changes between refinements. Also, there could be precision errors, as OpenFoam has only been set to output 6 significant figures. Finally, the FDE (finite difference equation) used to calculate the strain rate may be inaccurate, since we used a first-order forward/backward difference for the left and right walls. This was done since only two OpenFoam samples were taken at each wall per timestep, but that may not have been sufficient.

Assuming that the above is accurate, the net force on the internal beams comprising those walls can be calculated as follows (in units of  $\rho U^2 L^2$ ):

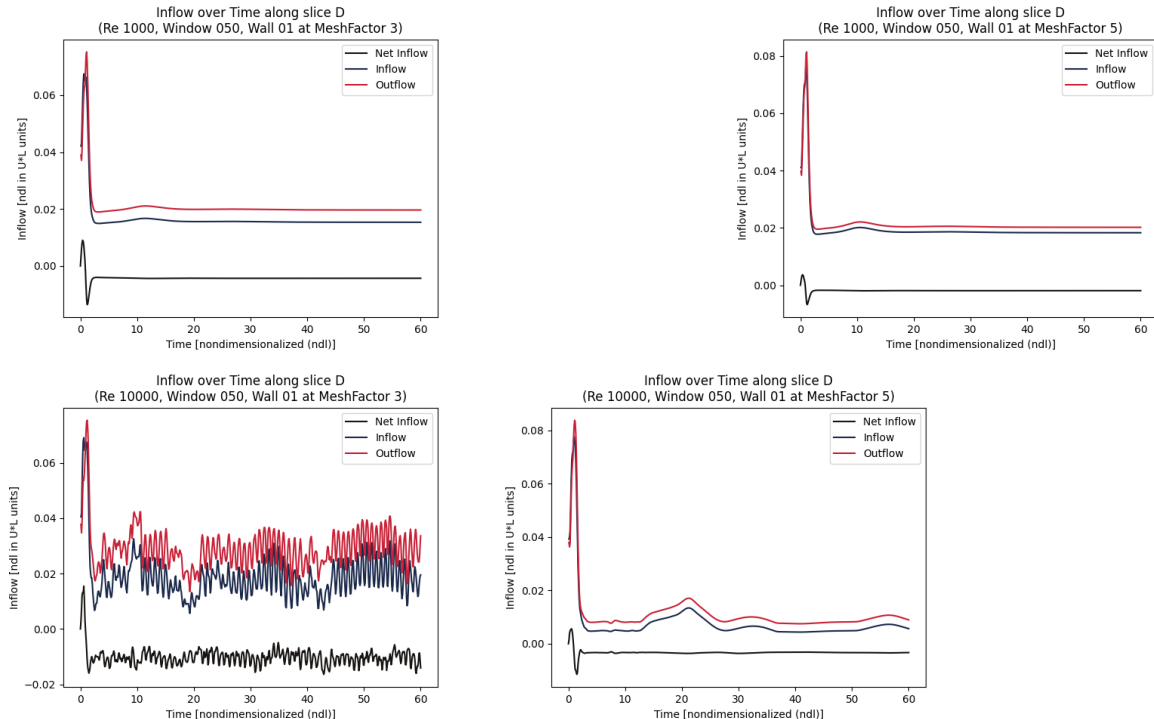
$$F = w * \tau = (0.1) * \tau = (0.1) * \mu * (\text{stress\_rate})$$

Since these results are fairly questionable, we do not calculate an example.

### 7.13. Volumetric Flow Rate and Mixing

To investigate inflow/outflow rates, we will consider integration of a profile across the internal window opening (profile D on the mesh diagram).

Note that the meshFactor of 3 fails for Re=10000 again.



Looking at the net flow rate, clearly the cavity first pressurizes and then slowly depressurizes over time.

While this is happening, large amounts of fluid are still being cycled through the window - a huge amount in the first few timesteps (up to  $\sim T=2$ ), and then a somewhat large amount afterwards.

To visualize the scale, an example will be shown.

For a  $1m^2$  window and  $90km/hr(56mph)$  wind, approximately  $(25m/s)(1)(1)(0.08) = 2m^3/second$  is cycled through in the first  $\sim 2$  seconds!  
Afterward,  $0.25m^3/s$  is cycled in and out on average.

After the initial spike, there is a net decreasing outflow starting at  $0.05m^3/s$  (using the Re=10000 plot).

Note this example is fairly realistic, since an EF0 tornado has slightly higher windspeed, and can be approximated as parallel streamline flow due to the large tornado radius.

While this example is not entirely accurate since the windspeed used can produce much higher Reynolds numbers in flow, the large-scale behavior is identical, as shown below.

Note that the maximum cycle flow rate of 8% freestream is consistent between both Reynolds numbers. From the previous analysis on Strouhal numbers, we see that since the large-scale flows are fairly Reynolds-number-independent, it is possible that the volumetric flowrate has converged, and will remain the same for higher Reynolds numbers.

If that is the case, then the low-Reynolds analysis can be combined with a couple of measurements of high-Reynolds flow, and extrapolated out to actual cases, providing an extremely useful tool for flow estimation.

A possible topic for further investigation would be the generation of fixed-Strouhal-number flow components with different Reynolds numbers. If the flow field can be separated into higher frequency harmonics that are added with higher Reynolds number, then that would allow modeling of higher Reynolds flow primarily with low-Reynolds measurements.

## 8. Conclusion

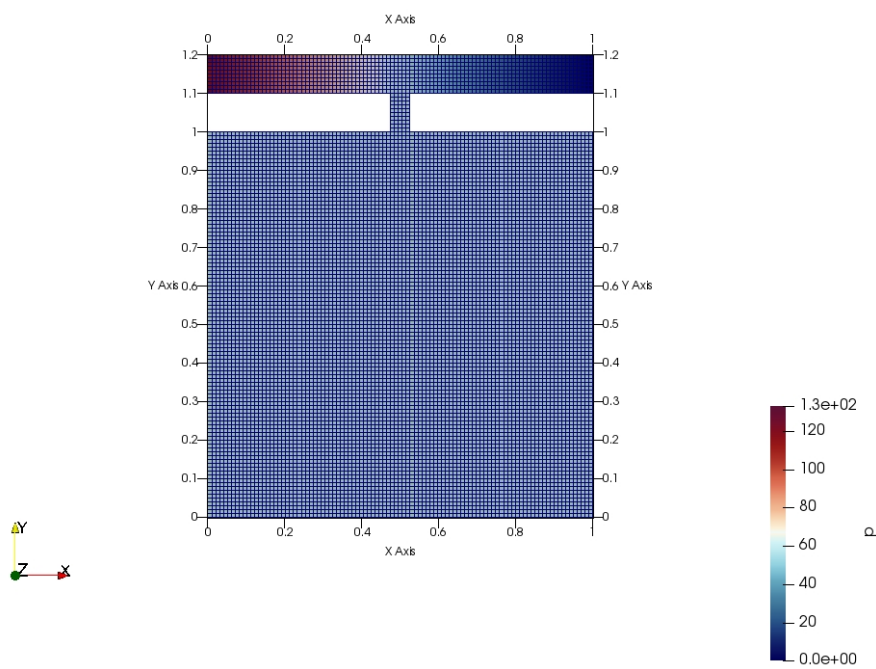
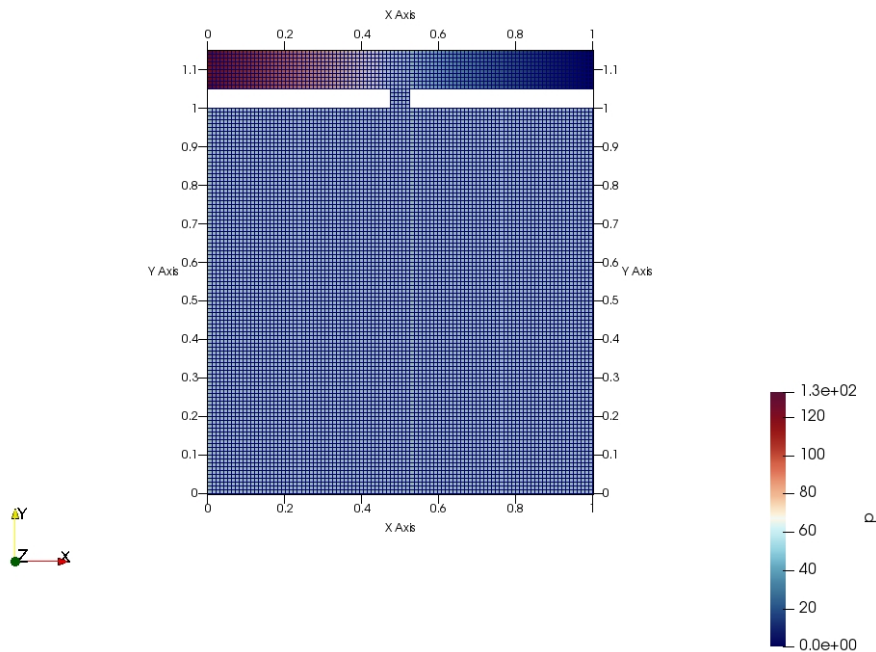
Cavities, or windows, in a structure when combined with external flow conditions with high airspeeds, may put undue stress on the structure on which the window is located. Intuitively, as reinforced by the simulations, a large window with a small wall thickness poses the least interference with the external flow conditions and would consequently equalize much more effectively than a small window with a large wall thickness. Although low airspeeds do not introduce catastrophic conditions for a structure, the equalization of conditions still introduces gradient flow conditions within the interior of the structure due to the zero-flow impermeability of the structure itself.

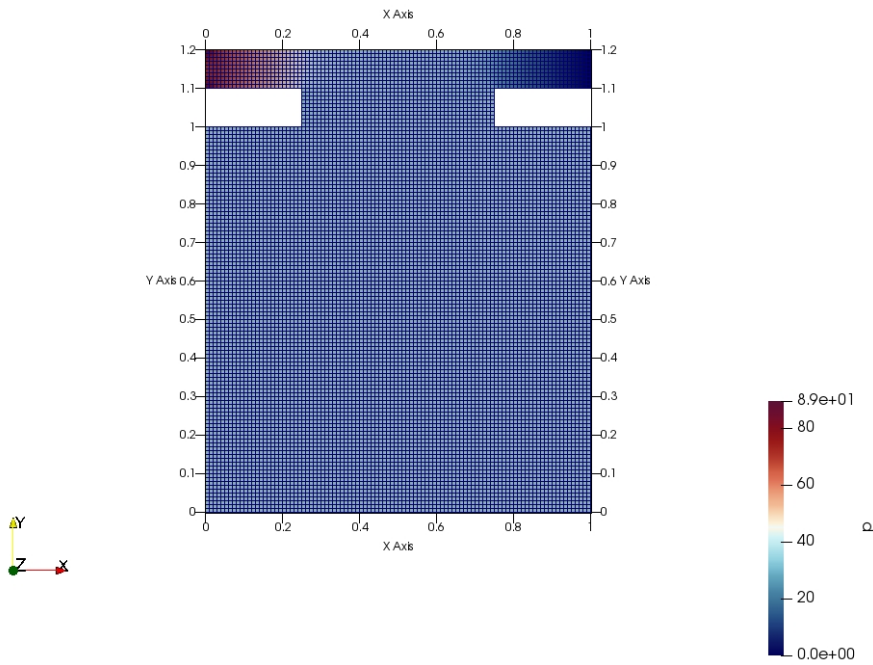
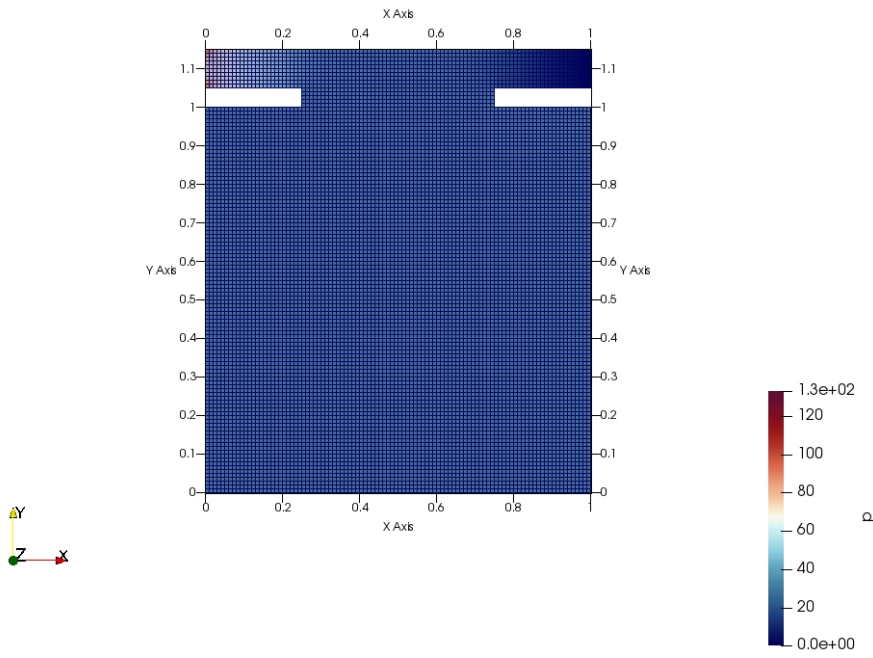
## 9. Appendix

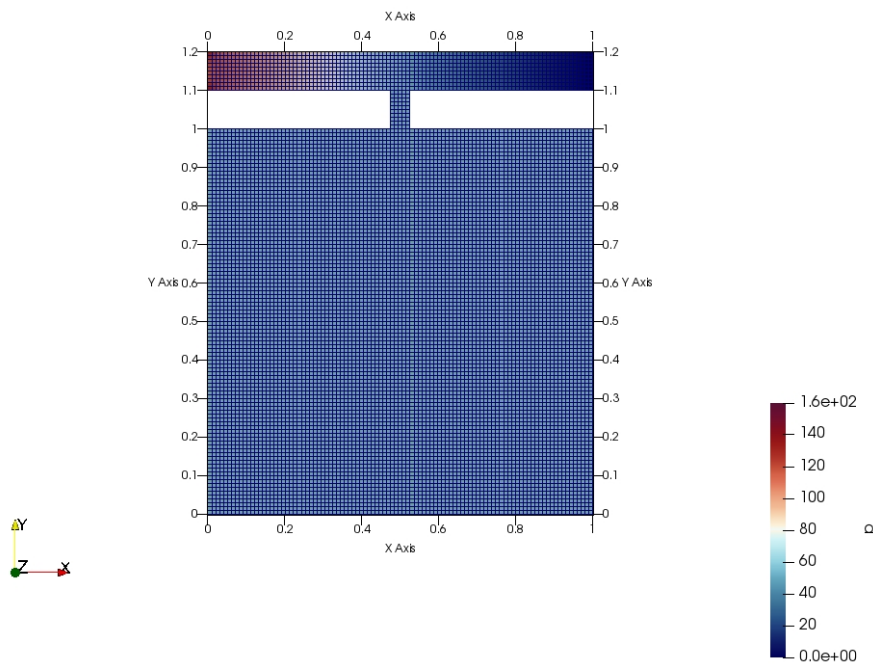
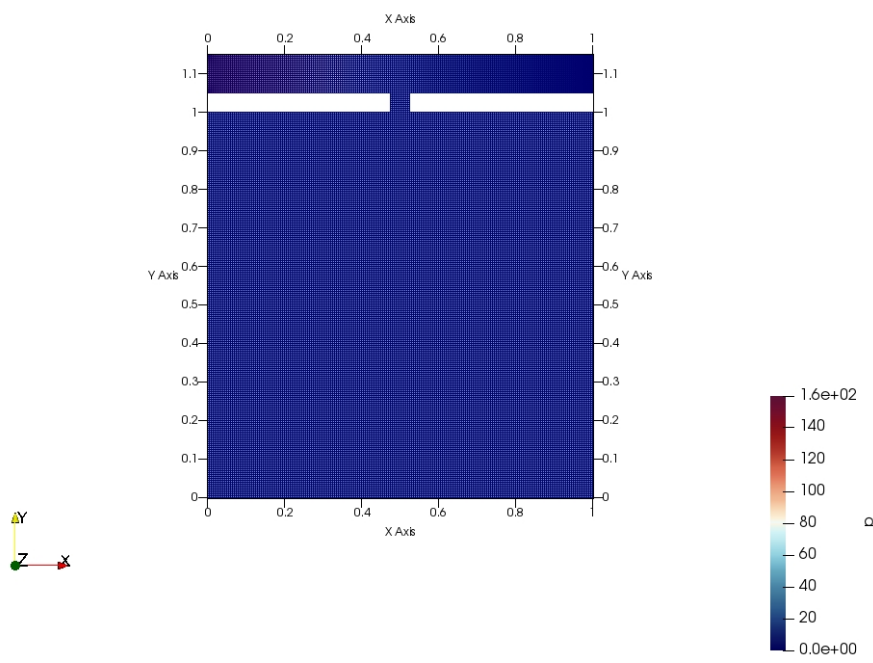
### 9.14. Mesh Images

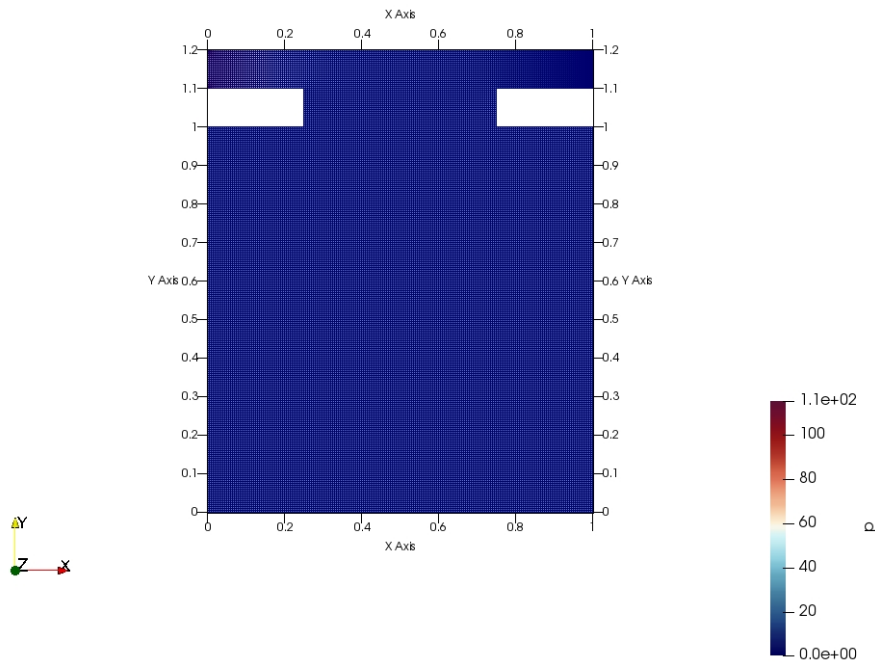
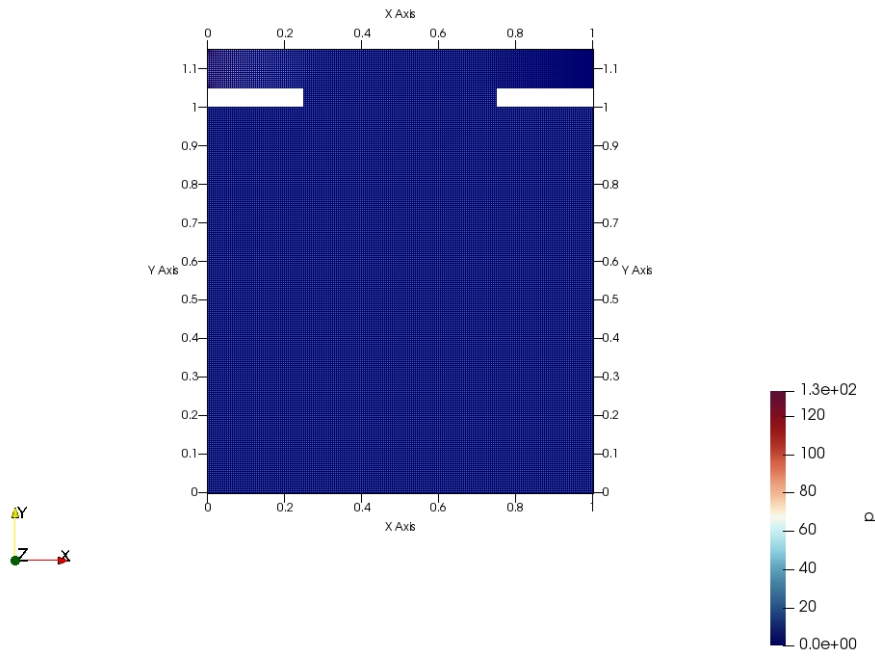
Below are the meshes for the various simulations that were conducted. The low Reynolds meshes varied both the width of the window and wall thickness to find patterns in flow behavior as an effect of those parameters.

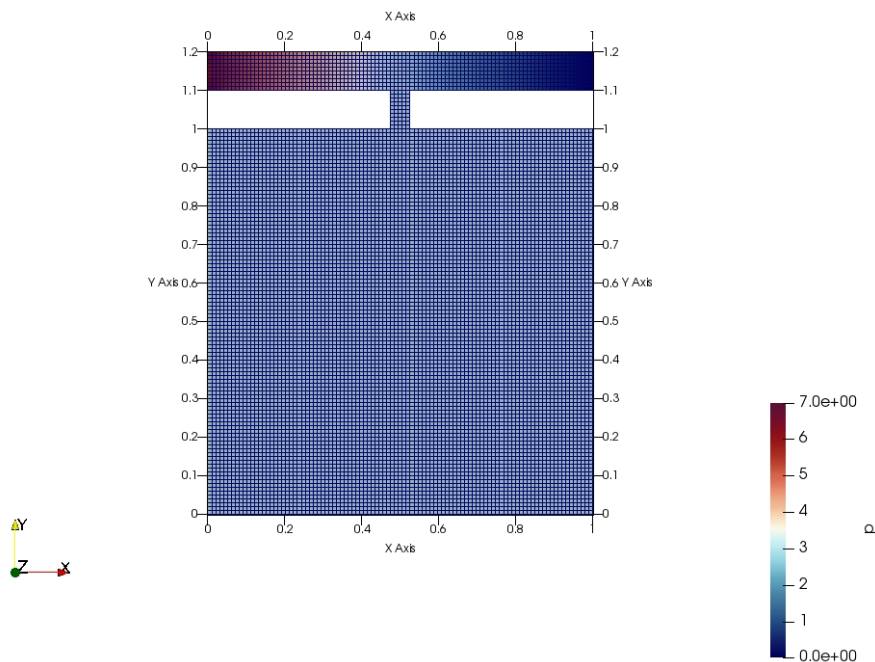
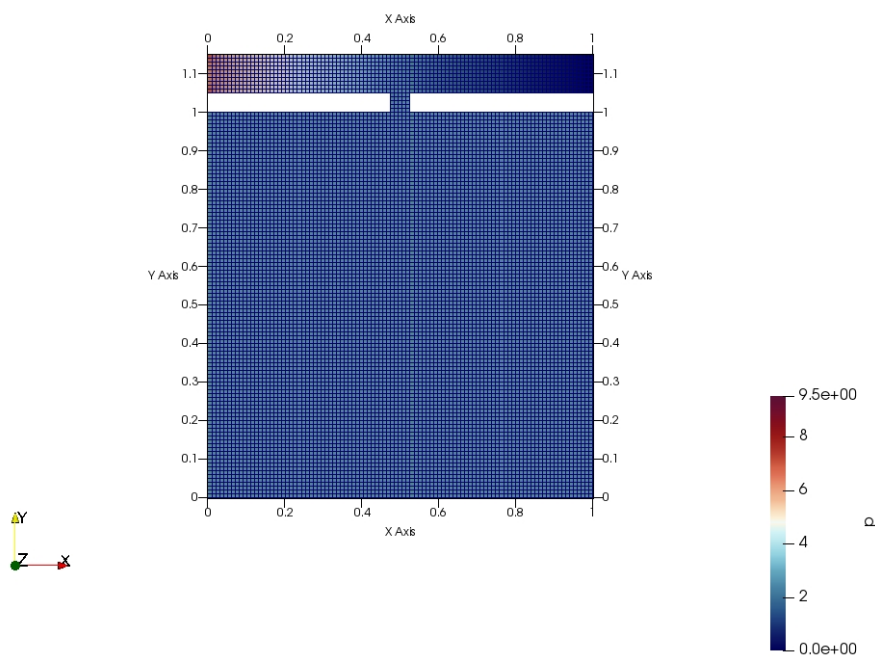
#### Mesh Images for the Low Reynolds simulations (same order)

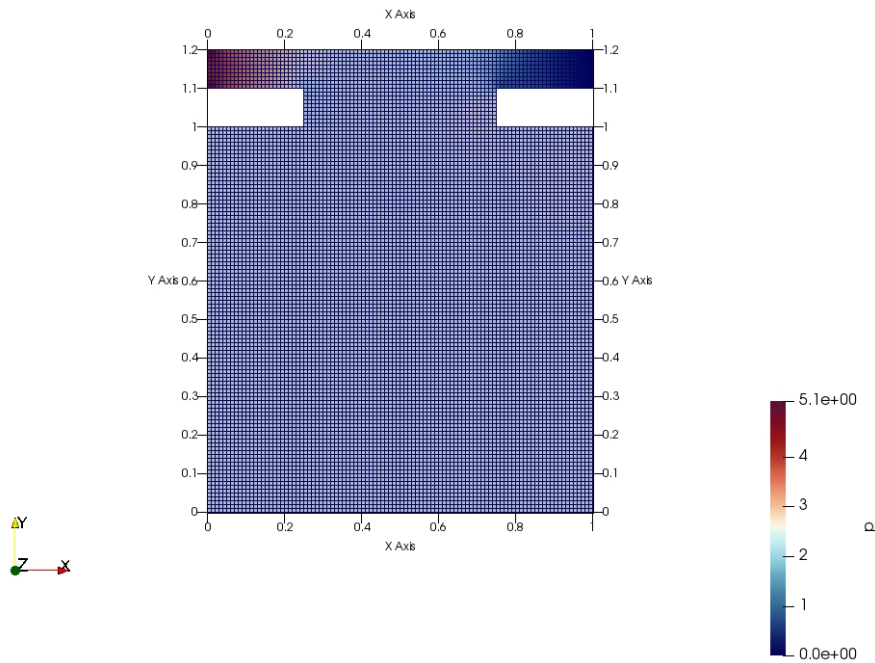
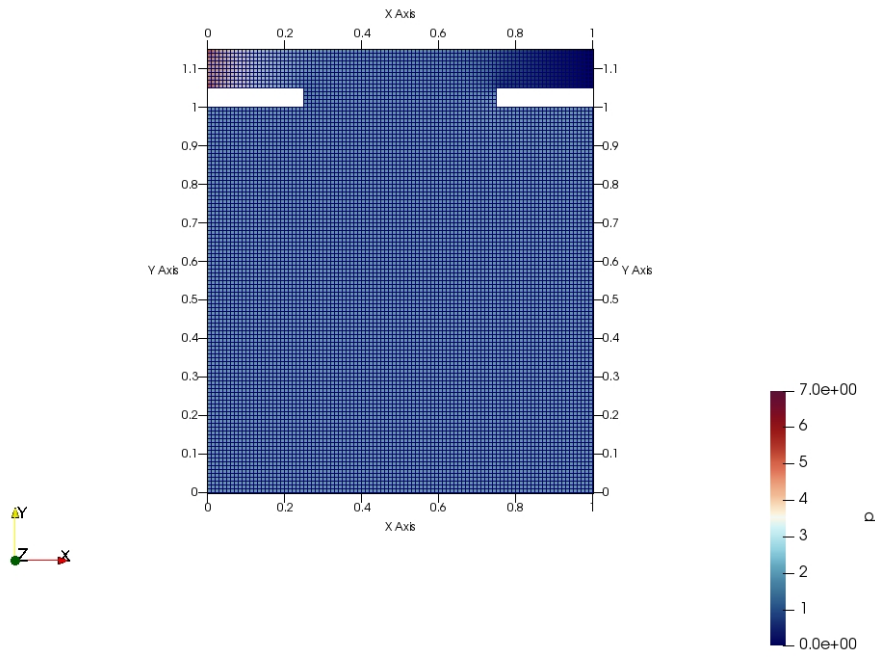


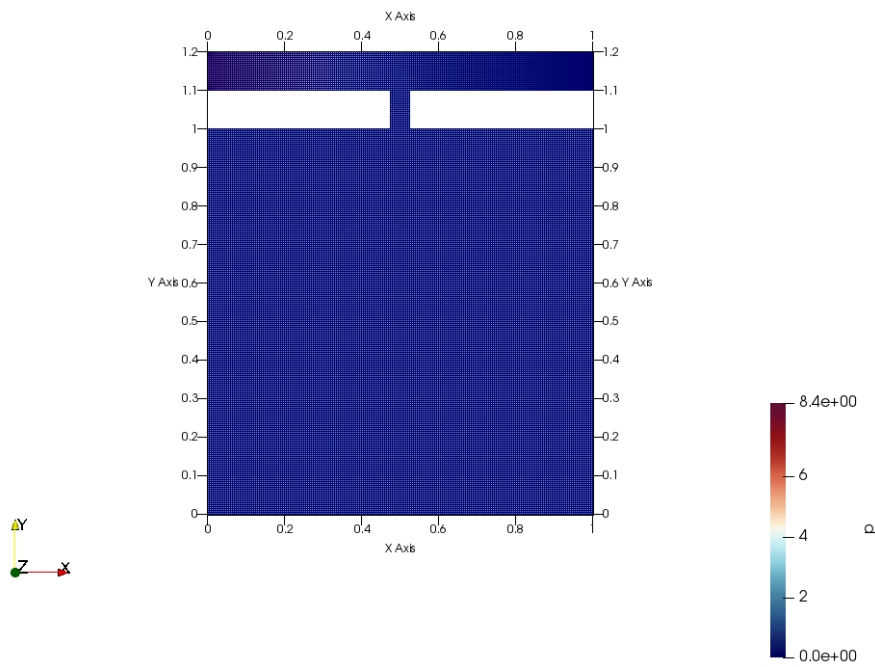
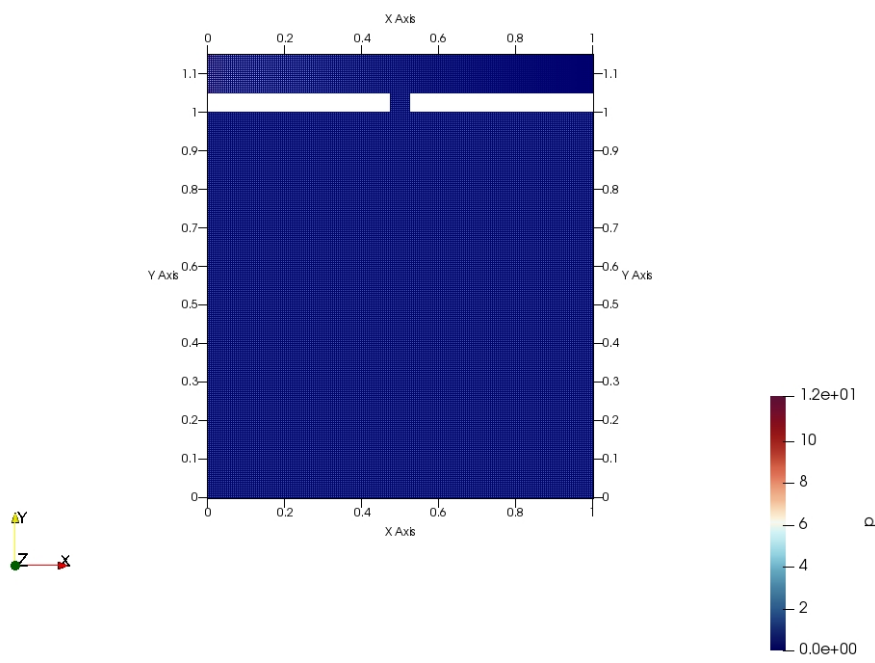


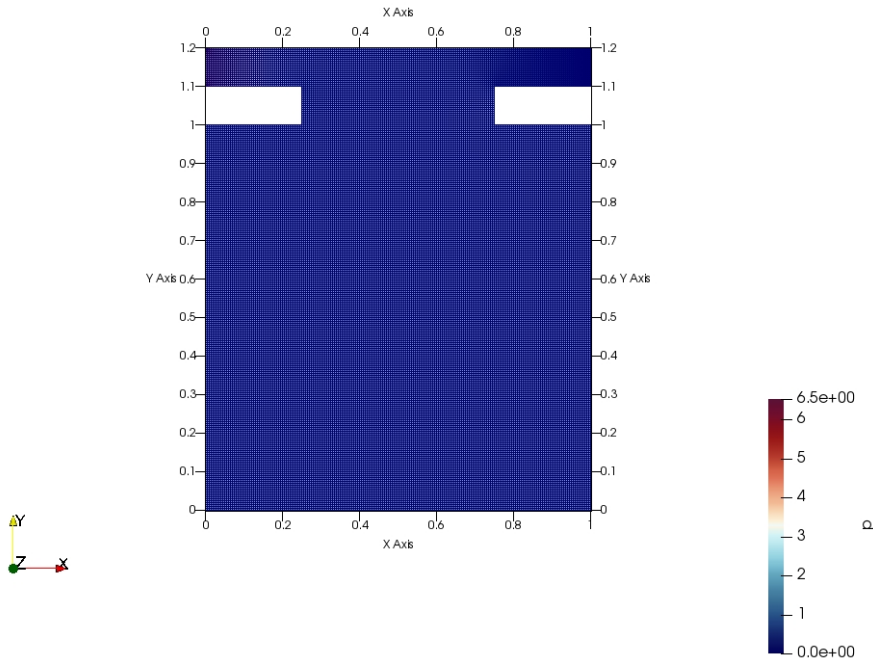
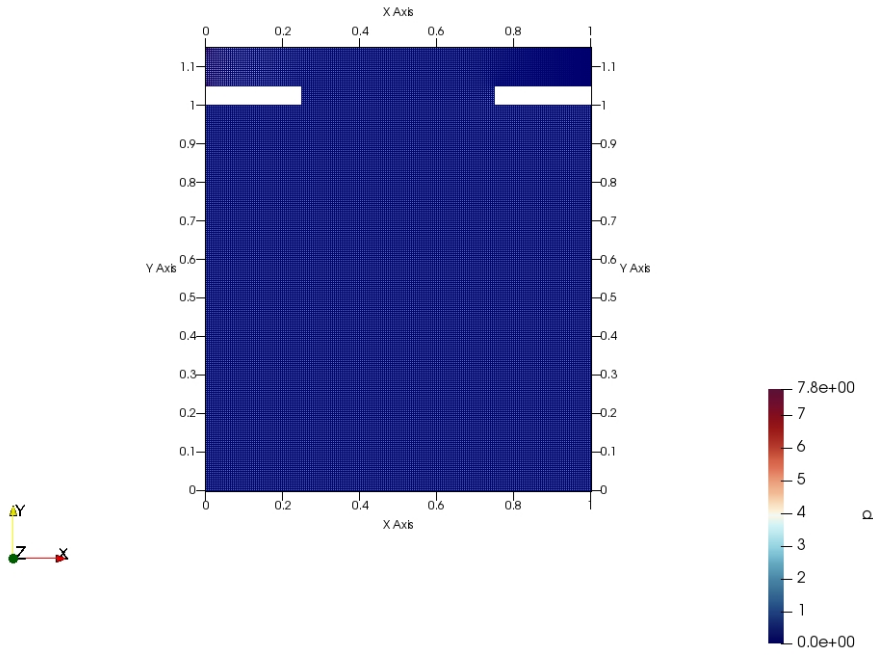






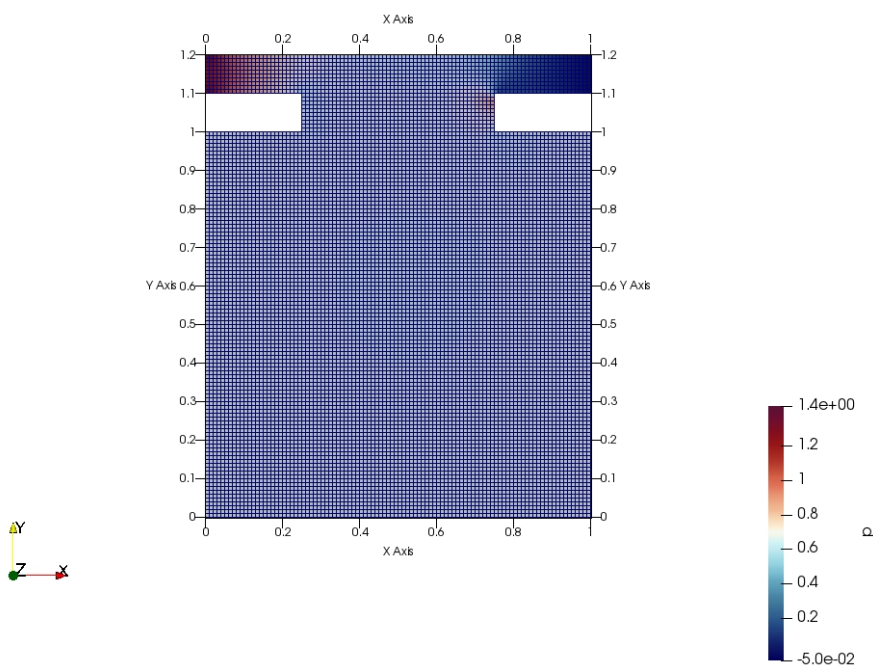
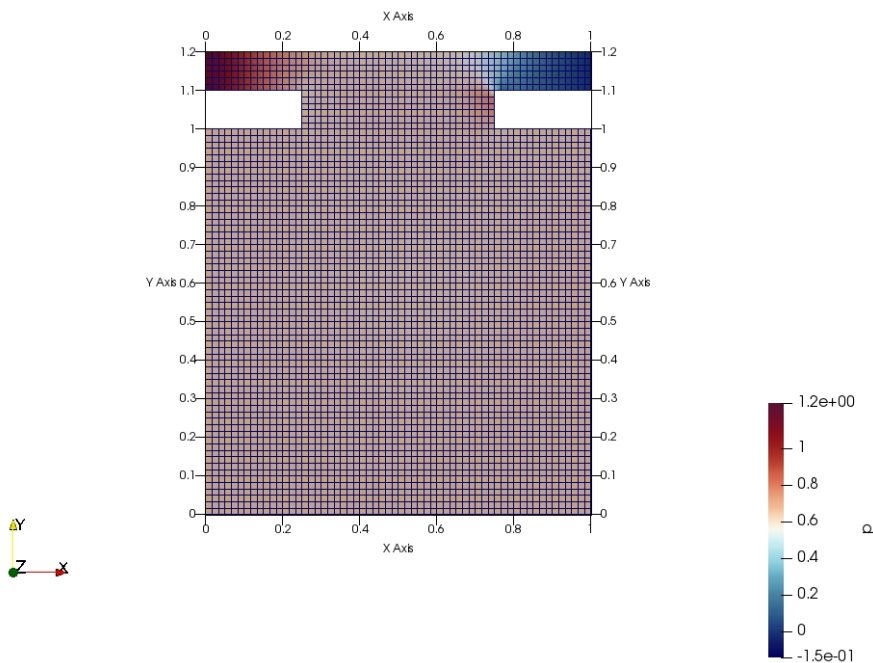


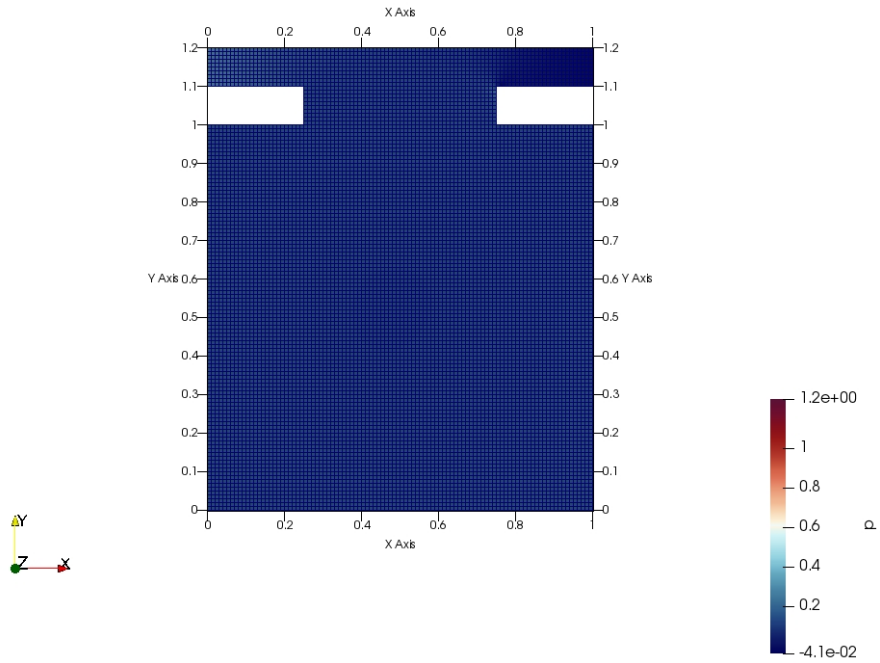
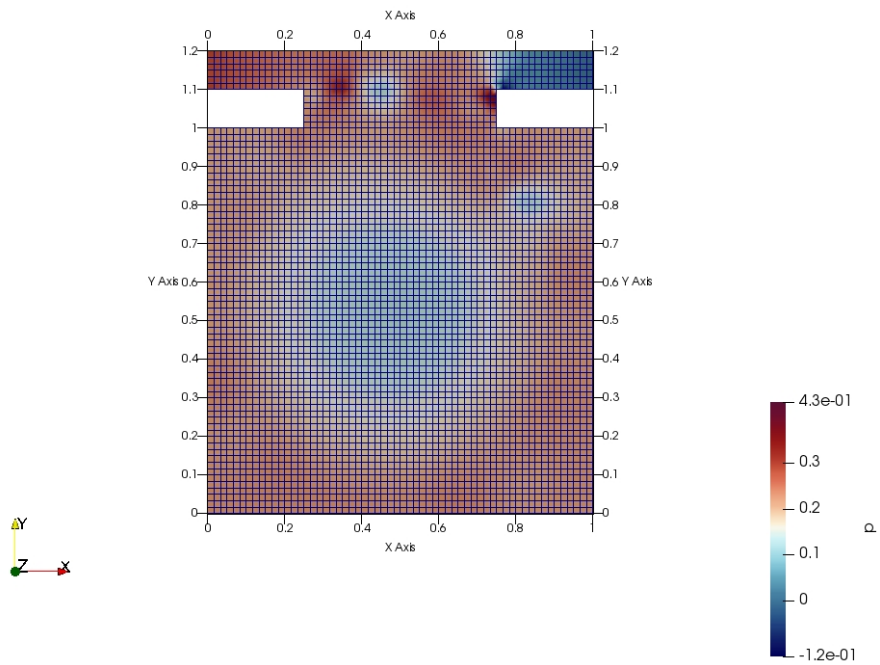




### **Mesh Images for the High Reynolds simulations (same order)**

The high Reynolds number meshes were used to find effects of high speed freestream airflow on the interior conditions of the cavity. For purposes of conciseness, the geometry of the meshes remained constant without variances in wall thickness nor window width.





## 10. References

(2019, May). *Super Inspection Pros*. Retrieved from <https://superinspectionpros.local:57400/blog/how-high-does-wind-speed-need-to-be-to-damage-a-home/>

- Allaire J, Xie Y, McPherson J, Luraschi J, Ushey K, Atkins A, Wickham H, Cheng J, Chang W, Iannone R (2021). *Rmarkdown: Dynamic Documents for r*. Retrieved from <https://CRAN.R-project.org/package=rmarkdown>
- Bengtsson H (2021). *R.utils: Various Programming Utilities*. Retrieved from <https://github.com/HenrikBengtsson/R.utils>
- Hadhazy A (2011, May). “How a Tornado Can Destroy a House.” *Popular Mechanics*. Retrieved from <https://www.popularmechanics.com/outdoors/survival/stories/gone-in-four-seconds-how-a-tornado-destroys-a-house>
- Kim HJ, Durbin PA (1988). “Observations of the Frequencies in a Sphere Wake and of Drag Increase by Acoustic Excitation.” *The Physics of Fluids*, **31**(11), 3260–3265. <https://doi.org/10.1063/1.8666937>.
- Sakamoto H, Haniu H (1990). “A study on vortex shedding from spheres in a uniform flow.” *ASME Journal of Fluids Engineering*, **112**, 386–392.
- Tessner T (2021, August). “What Are Hurricane Shutters? An Introduction to Hurricane Shutters.” *Eurex Shutters*. Retrieved from <https://eurexshutters.com/what-are-hurricane-shutters/>
- Urbanek S (2021). *Jpeg: Read and Write JPEG Images*. Retrieved from <http://www.rforge.net/jpeg/>
- Xie Y (2013). “animation: An R Package for Creating Animations and Demonstrating Statistical Methods.” *Journal of Statistical Software*, **53**(1), 1–27. Retrieved from <https://doi.org/10.18637/jss.v053.i01>
- Xie Y (2014). “Knitr: A Comprehensive Tool for Reproducible Research in R.” In *Implementing reproducible computational research*, eds. V Stodden, F Leisch, and RD Peng,. Chapman; Hall/CRC. Retrieved from <http://www.crcpress.com/product/isbn/9781466561595>
- Xie Y (2015). *Dynamic Documents with R and Knitr* 2nd ed. Chapman; Hall/CRC, Boca Raton, Florida. Retrieved from <https://yihui.org/knitr/>
- Xie Y (2021a). *Animation: A Gallery of Animations in Statistics and Utilities to Create Animations*. Retrieved from <https://yihui.org/animation/>
- Xie Y (2021b). *Knitr: A General-Purpose Package for Dynamic Report Generation in r*. Retrieved from <https://yihui.org/knitr/>
- Xie Y, Allaire JJ, Grolemund G (2018). *R Markdown: The Definitive Guide*. Chapman; Hall/CRC, Boca Raton, Florida. Retrieved from <https://bookdown.org/yihui/rmarkdown>
- Xie Y, Dervieux C, Riederer E (2020). *R Markdown Cookbook*. Chapman; Hall/CRC, Boca Raton, Florida. Retrieved from <https://bookdown.org/yihui/rmarkdown-cookbook>

## 11. Acknowledgements

Thank you so much for reading this work!

**Affiliation:**

Justin Campbell  
Aerospace Department, University of Texas at Austin  
E-mail: [Campbelljustin989@gmail.com](mailto:Campbelljustin989@gmail.com) - jsc4348

**Affiliation:**

Amanda Hiett  
Aerospace Department, University of Texas at Austin  
E-mail: [hiett.mandy@utexas.edu](mailto:hiett.mandy@utexas.edu) - amh7427

**Affiliation:**

Akhil Sadam  
Aerospace Department, University of Texas at Austin  
E-mail: [akhil.sadam@utexas.edu](mailto:akhil.sadam@utexas.edu) - as97822